ANNALS OF PHYSICS **189**, 53–88 (1989)

Physics of Projected Wavefunctions

CLAUDIUS GROS*

Institut für Theoretische Physik, ETH-Hönggerberg, 8093 Zürich, Switzerland

Received July 14, 1988

We present and discuss a variational approach to the one band Hubbard model in the limit of a large on-site Coulomb repulsion. The trial wavefunctions are the projected wavefunctions, generalized Gutzwiller wavefunctions. We discuss in detail the definition of these wavefunctions, the numerical methods used to evaluate them, their properties, and their physical relevance. Depending on the kind of parametrization used, the projected wavefunctions can describe a nearly localized Fermi liquid, an antiferromagnetically ordered state, or a quantum spin liquid. The physics of these three types of wavefunctions is described in detail. We discuss their relation to a proposed phase diagram of the two-dimensional Hubbard model and to results obtained by other approaches to the Hubbard model. The results obtained by numerical evaluation of the projected wavefunction are reviewed. The method used for the numerical evaluation, the variational Monte Carlo method, is described in detail. Finally we discuss the relation between a quantum spin liquid and the resonating valence bond state, which has been proposed, by P.W. Anderson, as a reference state for the Cu–O superconductors. In particular, we examine the question whether a quantum spin liquid is intrisically superconducting or not.

INTRODUCTION

The field of variational approaches to the one- and two-dimensional Hubbard and antiferromagnetic Heisenberg model is in rapid development. Recently, interest in these models increased further, when Anderson [1] suggested a close relation between these models and high temperature superconductors. Very recently, Birgeneau *et al.* [2] added additional experimental support to this point of view.

The physics of the two-dimensional Hubbard model is complex and far from being fully understood. As a function of the bandfilling and magnitude of the on-site Coulomb repulsion, ferro-, antiferro- and paramagnetic phases are expected. In Section 1 we give an introduction to the Hubbard model and discuss the relation between the antiferromagnetic Heisenberg Hamiltonian and the Hubbard model in the limit of large on-site Coulomb repulsion.

As fully interacting many-body systems, neither the Hubbard nor the Heisenberg Hamiltonian can be treated by standard many-body perturbation theory, since no

* Address after September 1, 1988: Department of Physics, University of Indiana, Swain Hall–West 117, Bloomington, IN 47405.

0003-4916/89 $7.50

small parameters are present. The variational approach to these models has therefore been intensively followed, since it is one of a few nonperturbative methodes available in this context. In Section 2 we first give a short overview over some methods in use to approach the Hubbard Hamiltonian and then introduce and discuss in detail the trial wavefunctions we use for our variational approach. These are the *projected wavefunctions*, generalized Gutzwiller wavefunctions. Exploiting fully the variational degree of freedom of the projected wavefunctions, they can potentially describe both the para- and the antiferromagnetic region of phase space.

The calculation of the properties of these wavefunctions is not straightforward. A *variational Monte Carlo* method must be used to evaluate the properties of the projected wavefunctions numerically. This method is presented and discussed thoroughly in Section 3. The problem of the extrapolation of results obtained for finite lattice to the thermodynamic limit is discussed in this context.

Then, in Section 4, the properties and the physics of the projected wavefunctions in one and two dimensions are discussed in detail. This is done with the help of results obtained by the variational Monte Carlo method. With respect to the results obtained for one dimension, we discuss the concept of a *nearly localized Fermi liquid.* We then show that a certain projected wavefunction, the projected Fermi sea, should give a good description of this state. In two dimensions we focus on the concept of a *quantum spin liquid* and discuss its relation to the *resonating valence bond* state, introduced by Anderson [1]. We show that the projected *d*-wave BCS wave function is a good candidate for a quantum spin liquid. This would then mean that a quantum spin liquid is intrinsically superconducting, with possible relevance for the high temperature superconductors.

Section 1. The Hubbard Model

1. *Introduction to the Hubbard Hamiltonian*

We begin with a short introduction to the Hubbard model. The Hubbard model describes fermions with only one orbital degree of freedom and spin $\frac{1}{2}$, when the on-site Coulomb interaction in a tight binding description is dominant.

Let us denote by $c_{i,\sigma}^{+}$ the Fermion creation operator on site i with spin $\sigma = \downarrow, \uparrow$. The Hubbard Hamiltonian then takes the form

$$H = -\sum_{\langle i,j\rangle,\sigma} t_{i,j}(c_{i,\sigma}^{+}c_{j,\sigma} + c_{j,\sigma}^{+}c_{i,\sigma}) + U\sum_{i} n_{i,\downarrow}n_{i,\uparrow}. \tag{1}$$

Here, the $t_{i,j}$ are the one-particle hopping matrix elements and $U > 0$ is the on-site correlation energy.

We define by $c_{\mathbf{k},\sigma}^{+} = 1/\sqrt{L}\sum_{\mathbf{R}} e^{i\mathbf{R}\mathbf{k}} c_{\mathbf{R},\sigma}^{+}$ the creation operator in $\mathbf{k}$-space. L is the

total number of lattice sites, for a finite lattice with periodic boundary conditions. The kinetic energy takes then the form

$$T = \sum_{\mathbf{k},\sigma} \varepsilon(\mathbf{k})\, c^{+}_{\mathbf{k},\sigma} c_{\mathbf{k},\sigma}$$
$$\varepsilon(\mathbf{k}) = -1/L \sum_{\mathbf{R},\mathbf{R}'} e^{i(\mathbf{R}-\mathbf{R}')\cdot\mathbf{k}} t_{\mathbf{R},\mathbf{R}'}. \tag{2}$$

Throughout this paper, we will mainly consider the case where $t_{i,j} = t > 0$ for $\langle i, j \rangle$ nearest-neighbor (n.n.) sites, and zero otherwise. For a two-dimensional (dim) square lattice, $\varepsilon(\mathbf{k})$ takes the form

$$\varepsilon(\mathbf{k}) = -2t(\cos(k_x) + \cos(k_y)). \tag{3}$$

Here k_x and k_x are the x, y-components of $\mathbf{k}$ and the lattice parameter is set equal to 1. The generalization of $\varepsilon(\mathbf{k})$ to different lattices is straightforward. In Fig. 1, the density of states and the Fermi surfaces are shown for various band fillings, n, in two dimensions.

For the half-filled case ($n = 1$), the Fermi surface is perfectly nesting; i.e., the Fermi surface is invariant with respect to a translation by $Q = (\pi, \pi)$, which is half a reciprocal lattice vector. This is true also in one and three dimensions, for certain lattices. Therefore, for $n = 1$, the system is subject to an antiferromagnetic instability for arbitrary small values of U. This can be seen, e.g., in RPA approximation [3]. A gap will open at the Fermi surface and the system will be an insulator for all ratios of t/U, at zero temperature. For a more general band structure $\varepsilon(\mathbf{k})$, we expect that

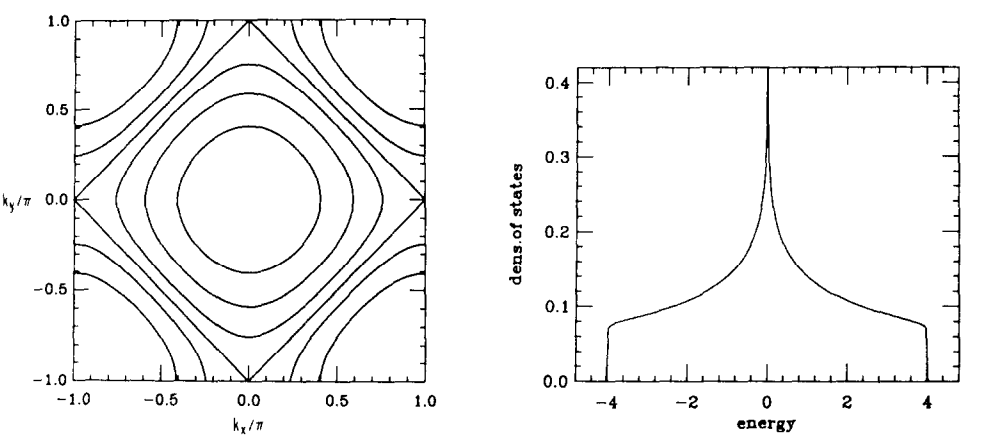

FIG. 1. (Left) Fermi surface of electrons on a two-dimensional square lattice with nearest-neighbor hopping only. Band fillings are $n = 0.25, 0.5, ..., 1.5$, starting from the inner surface. Note that the Fermi surface for the half-filled case is perfectly nesting. (Right) Density of states for noninteracting electrons on a two-dimensional square lattice with nearest-heighbor hopping only. The singularity at the origin is logarithmic. Both figures are taken from Ref. [3].

the system will remain metallic for small U. Only when U becomes larger than critical U (U_c) of the order of the bandwidth W, is a transition to a Mott insulator [4] expected. In magnetically nonfrustrated systems, this transition should be accompanied by antiferromagnetic ordering. In a frustrated system, however, this could be a transition from a paramagnetic metal to paramagnetic insulator.

The frustration can arise from two sources: it can be a lattice effect; i.e., a fcc or triangular lattice with only n.n. interaction is frustrated, or it can be a consequence of competing interaction between, e.g., n.n. and next-nearest-neighbor (n.n.n.) interactions. In this case, the Hamiltonian (Eq. (1)) would have a large n.n.n. hopping term in addition to the n.n. term. The effects resulting from frustration are discussed further in the next two sections.

2. *Large U Expansion*

For the remaining part of this paper, we will consider what happens when U is large. With large U one generally means that U should be much larger than the bandwidth $W = 2zt$. Here z is the number of n.n. sites. In Section 1.5 we discuss in more detail what large U means with respect to the Mott critical U_c.

In the limit of large on-site repulsion U, real doubly occupied sites are energetically very unfavourable and therefore suppressed. Only virtual doubly occupied sites will be present, i.e., they will be bound to a nearby empty site, as we explain in Section 1.5.

The most convenient way of treating these virtual doubly occupied sites is to perform a unitary transformation on the Hilbert space, e^{iS}, which eliminates high energy processes in lowest order in t/U. These are hopping processes, which change the total number of doubly occupied sites, as illustrated in Fig. 2.

The other hopping processes, which do not change the number of doubly

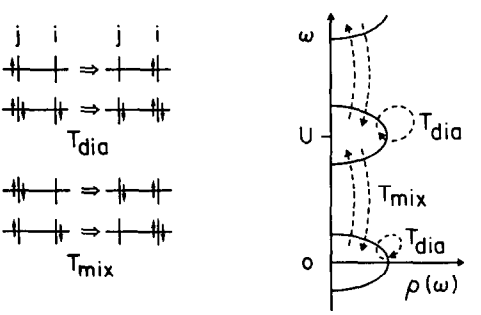

FIG. 2. Principles for the canonical transformation, which leads from the Hubbard Hamiltonian to H_{eff}. (Left) The kinetic energy operator T is split, with respect to the total number of doubly occupied sites, into a diagonal (T_{dia}) and a nondiagonal (T_{mix}) term. (Right) The lowest Hubbard bands, which are defined by the density of states of (T_{dia}). For large on-site repulsion U, the different Hubbard bands are well separated. Therefore T_{mix} correspond to high energy process and can be treated in perturbation theory, while T_{dia} describes low energy processes.

occupied sites, are low energy processes and will be retained in the transformed Hamiltonian

$$\begin{aligned} H_{\text{eff}} &= e^{iS} H e^{-iS} \\ &= H + i[S, H] + i^2/2[S, [S, H]] + \cdots . \end{aligned} \tag{4}$$

Up to second order in t/U, H_{eff} takes the form [5].

$$\begin{aligned} H_{\text{eff}} &= T + H_{\text{eff}}^{(2)} + H_{\text{eff}}^{(3)}, \\ T &= -t \sum_{\langle i,j\rangle,\sigma} (a_{i,\sigma}^{+} a_{j,\sigma} + a_{j,\sigma}^{+} a_{i,\sigma}) \\ H_{\text{eff}}^{(2)} &= 4t^2/U \sum_{\langle i,j\rangle} (\mathbf{S}_i \cdot \mathbf{S}_j - n_i n_j/4) \\ H_{\text{eff}}^{(3)} &= -t^2/U \sum_{i,\tau\neq\tau',\sigma} (a_{i+\tau,\sigma}^{+} a_{i,-\sigma}^{+} a_{i,-\sigma} a_{i+\tau',\sigma} + a_{i+\tau,-\sigma}^{+} a_{i,\sigma}^{+} a_{i,-\sigma} a_{i+\tau',\sigma}). \end{aligned} \tag{5}$$

Here $\mathbf{S}_i$ are the spin operators on site i, $a_{i,\sigma}^{+} = (1 - n_{i,-\sigma})\, c_{i,\sigma}^{+}$ with $n_i = n_{i,\downarrow} + n_{i,\uparrow}$, $n_{i,\sigma} = c_{i,\sigma}^{+} c_{i,\sigma}$. $\langle i, j\rangle$ are pairs of n.n. sites and $i+\tau$ denotes a n.n. site of i. T is the kinetic energy of the holes and $H_{\text{eff}}^{(2,3)}$ the two- and three-site contributions, respectively.

This effective Hamiltonian is valid only in the subspace of no doubly occupied sites, since it corresponds to the first terms of a perturbation expansion in t/U in this subspace. In the half-filled case, H_{eff} reduces to the antiferromagnetic Heisenberg Hamiltonion (AFH), with a n.n. coupling constant $J = 4t^2/U$. In this limit, H_{eff} depends crucially on the band structure [6]. If a n.n.n. hopping term is present in (1), then we would have to add to H_{eff} a n.n.n. antiferromagnetic spin–spin coupling term. If this term is large, then the resulting model will be frustrated.

3. *Case of Infinite U*

H_{eff}, as given by (5), corresponds to the first terms of an infinite expansion series in t/U. Before we discuss the convergence radius of this series and the quality of the approximation (5), we consider the limit $t/U \to 0$, where this expansion is surely valid.

In this limit, only the kinetic energy term for the holes survives in the expansion for H_{eff}. When no holes are present, the Hamiltonian is identically zero, and all 2^L states are degenerate. When a few holes are present, one interesting question is whether the ground state is paramagnetic or ferromagnetic. Nagaoka [7] showed that for exactly one hole, the system is ferromagnetically ordered, when the lattice is nonfrustrated.

The physical reason for this *Nagaoka effect* is the following: When all spins point in one direction, the hole can move freely and has therefore minimal kinetic energy. On the other hand, when the spins point randomly in every direction, the holes disturbs the local spin configuration while it propagates and one expects a reduction of the bandwidth.

The Nagaoka effect is very sensitive to the form of the band structure. The argument we present in the following has been pointed out by Einnarson [8].

The density of states for a system with one hole can be calculated by a moment expansion of the diagonal part of the real space hole–hole Greens-function [9]. This moment expansion can be done for different background spin configurations. The spin configuration around the hole can be ferro-, para-, or antiferromagnetic. By a calculation and comparison of the lower band edge, for one hole in one of these three different spin configurations, one can decide which is energetically favourable.

We now consider a square lattice with n.n. $(-t_1)$ and n.n.n. $(-t_2)$ hopping matrix elements and $U=\infty$. Only those paths contribute to the diagonal part of the hole–hole Greens function, in which the hole returns to its initial site. Of these paths, the most important are the self-retracing paths [9]. These are paths where the hole hops exactly the same way backwards and forwards, as illustrated in Fig. 3(a). All these self-retracing paths give a positive contribution to the Greens-function; $(-t_1)^{2n}(-t_2)^{2m}$, where n, m are integers.

For non-self-retracing paths, like those illustrated in Figs. 3(b) and 3(c), destructive interference might arise whenever $-t_2$ is negative. (Note that $-t_1$ and $-t_2$ are defined as the hopping matrix elements in Eq. (1).) The paths illustrated in Figs. 3(b) and 3(c) contribute a term $\sim(-t_1)^2(-t_2)$ to the hole–hole Greens-function. This contribution is destructive, when $t_2>0$. This path contributes in the ferromagnetic case (Fig. 3(c)) but not in the antiferromagnetic case (Fig. 3(b)), since in this case the spin configuration is not the same at the end as in the beginning.

The occurrence of destructive interference depends only on the absolute sign of

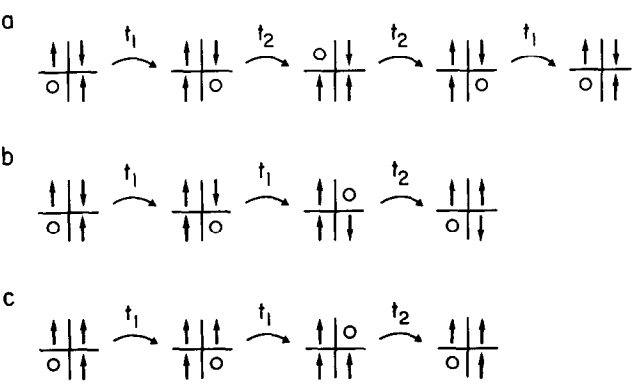

FIG. 3. Illustration of some paths contributing to the diagonal hole–hole Greens-function for infinite U and nearest-neighbor $(-t_1)$ and next-nearest-neighbor $(-t_2)$ hopping. (a) A self-retracing paths of order $(-t_1)^2(-t_2)^2$. Note that the spin configuration is restored at the end. (b) and (c) A non-self-retracing path of order $(-t_1)^2(-t_2)$ for an antiferro- and a ferromagnetic spin configuration, respectively. Note that the spin configuration is restored for the ferro- but not for the antiferromagnetic case.

t_2. In a t_1 hop, the hole changes A–B sublattice, but not i a t_2 process. Any contributing path contains therefore an even number of t_1 processes.

This destructive interference, for $t_2 > 0$ in the ferromagnetic case, is an indication that the ground state might be antiferro- or paramagnetic if t_2 is large enough.

4. *Convergence Radius of* H_{eff}

Now we discuss in some detail the convergence radius for the expansion of $H_{\text{eff}} = e^{iS} H e^{-iS}$ in t/U. S is determined by requiring that in H_{eff} no terms which mix different Hubbard bands should be present, i.e., states with different numbers of doubly occupied sites. This can be done recursively in each order of t/U, by expanding S in t/U. This transformation corresponds to an infinite perturbation expansion within the subspace of no doubly occupied sites.

Whereas the Hamiltonian transforms according to $H_{\text{eff}} = e^{iS} H e^{-iS}$, the wavefunctions transform like $|\psi_{\text{eff}}\rangle = e^{iS} |\psi\rangle$. Here $|\psi_{\text{eff}}\rangle$ has a fixed number of doubly occupied sites; i.e., it is an eigenstate of $\sum_i n_{i,\downarrow} n_{i,\uparrow}$. Within an exact approach it is equivalent [10] to work with H_{eff} and $|\psi_{\text{eff}}\rangle$, or with H and $|\psi\rangle$.

Now, when the expansion for H_{eff} converges for $n = 1$, we are dealing with a system with a Mott insulator ground state, since we are doing perturbation about a localized state. In terms of the original Hilbert space, this means that doubly occupied and empty sites are bound [5]. d.c. conductivity is therefore zero, since these excitons of doubly occupied and empty sites are neutral. Therefore we expect that, for $n = 1$, the expansion series for H_{eff} converges for all $U > U_c$.

For the Hubbard model with n.n. hopping only, the situation is special. No Mott transition is expected and the ground state should be insulating for all ratios of t/U, in the half-filled case. This is surely true in one dim, where the exact solution is known [11]. In two and three dim, this is expected to be a consequence of the perfectly nesting properties of the Fermi surface at half filling. The antiferromagnetisms for both large and small U, are commensurate with the lattice spacing. A continuous transition from small to large U is expected.

The convergence radius of H_{eff} should therefore be infinite in this case. Physically, this means that the properties of the system vary smoothly with t/U. In this situation, we expect that the approximation of H_{eff} by Eq. (5), i.e., by the terms up to second order in t/U, should be quite good for values of U down to about the bandwidth.

Since H_{eff}, $|\psi_{\text{eff}}\rangle$ and H, $|\psi\rangle$ are related by means of a unitary transformation, within an exact approach, it is equivalent to work with either the transformed or the original Hilbert space. In a variational approach, this is no longer true. In the original Hilbert space, the variational wavefunctions should have bound empty and doubly occupied sites, in order to describe correctly the physics of the ground state. Such wavefunctions are very difficult to write down. On the other hand, a straightforward procedure exists to construct trial wavefunctions with no doubly occupied sites, as necessary for the ground state of H_{eff}. This can be done by a projection operator, as we explain in detail in Section 2. It is therefore much more convenient, in a variational approach, to work in the transformed Hilbert space.

The backwards transformed wavefunction, $|\psi\rangle = \exp(-iS)\,|\psi_{\text{eff}}\rangle$, has then automatically bound empty and doubly occupied sites.

Another reason for a broken equivalence between the two Hilbert spaces is of course the approximation of H_{eff} by the first two terms in t/U expansion (Eq. (5)). Only when the complete perturbation series is taken into account, is the equivalence exact.

5. *Phase Diagram*

Up to now, we have discussed the physics of the Hubbard model only exactly on the axes in a $(1-n)$ versus t/U phase diagram. We now take a look at the whole phase diagram. Concretely, we consider H_{eff} on the two-dim square lattice with n.n. interactions only.

At finite temperature, long range magnetic [12] or superconducting [13] (s.c.) order is not possible in this model, since a continuous symmetry cannot be broken in two dimensions at finite temperatures. But for a system with weakly coupled layers, a *quasi-two-dim* system, a true three-dim phase transition can occur at finite temperatures, driven by the in-plane fluctuations. We consider such a system in what follows.

In Fig. 4 we show the phase diagram. It is not clear to which doping concentrations, $\delta_C = (1-n_C)$, the antiferrromagnetic phase (AF) extends, and whether δ_C is finite. The extension of the ferromagnetic phase (F) to finite δ is still unclear.

For very small particle concentrations $n \ll 1$, the kinetic energy $(\sim -nt)$ dominates with respect to the interaction energy $(\sim -n^2 J)$, since the interaction is short ranged. We expect therefore Fermi liquid behavior at low temperatures compared to the Fermi temperature [14]. Whether this Fermi liquid is unstable against s.c. pairing, due to the residual interactions, is unclear. If so, the transition will be BCS-like, since the system scales to the weak coupling (w.c.) limit for $n \to 0$. Note that this behaviour is opposite that of the free electron gas, where the interaction is long ranged and dominates at low densities.

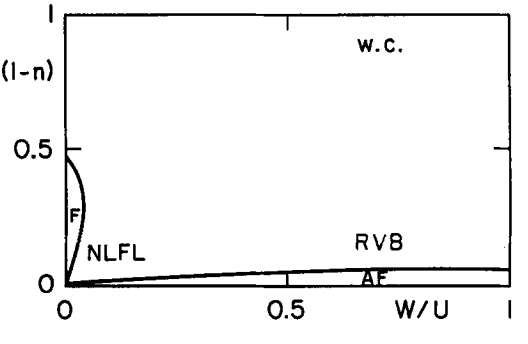

FIG. 4. Phase diagram for the two-dimensional Hubbard model with nearest-neighbor hopping only. Here n is the density of particles, $W = 2zt$ the bandwith, and U the on-site repulsion energy. The abbreviations are F for ferromagnetic, AF for antiferromagnetic, NLFL for nearly localized Fermi liquid, RVB for reasonating valence bond state, and w.c. for weak coupling regime.

Now we examine the region where $(1-n) \ll 1$, but large enough to avoid the antiferromagnetic instability. For these densities the properties of the system depend very strongly on the relative value of the kinetic to that of the interaction energy. We estimate both contributions as follows: For small doping concentrations, the kinetic energy per hole is about $-\alpha zt$, with α corresponding to the reduction of the bandwidth by the interaction ($0.5 < \alpha < 1.0 < 1.0$ [9]). The interaction energy can be approximated by the two-site contributions, which are dominant for small doping. In order of magnitude $\langle \mathbf{S}_i \cdot \mathbf{S}_j \rangle \sim -\frac{1}{4}$, so that the total energy per site sums to $-(1-n)\,\alpha zt - 0.5zt^2/U$. Two limits are possible.

First, if $t/U \ll 2\alpha(1-n)$, then we are in the regime of a *nearly localized Fermi liquid* (NLFL). It is a Fermi liquid, with a strongly renormalized Fermi temperature $T_F^* \sim (1-n)T_F$ and strong short range antiferromagnetic spin–spin correlations [10]. These antiferromagnetic correlations are however not a consequence of the magnetic interaction, but are due to the strong on-site correlation, i.e., the exclusion of doubly occupied sites. Furthermore, these correlations will disappear at a temperature scale of T_F^*. The NLFL is close to both the ferro- and the antiferromagnetic phase. In Section 4.2 we argue that physically the NLFL is nearly antiferromagnetic and not nearly ferromagnetic and that the transition to the ferromagnetic phase should be of first order.

On the other hand, if $2\alpha(1-n) \sim t/U$, then the antiferromagnetic interaction is dominating. We also have short range antiferromagnetic spin–spin correlations, but of different origin, due to the interaction. They disappear only at a temperature scale of J. The nature of this state is complety different from that of a Fermi liquid. Anderson proposed [1] that it is a new quantum liquid state, which he called a *resonating valence bond* (RVB) state. In particular, he suggested that this state might show superconductivity with a very high transition temperature, determined by J.

In the following, we try to describe these two states, NLFL and RVB, by variational wavefunctions. In Fig. 4, no boundary is drawn between the RVB and the NLFL state. Within our approach by variational wavefunctions, we argue (Section 4) that the ground state of the RVB state is superconducting. Our trial wavefunction for the NLFL is on the other hand a Fermi liquid wavefunction. It is unclear whether this state is unstable against s.c. due to the residual spin–spin interactions. If so, we would expect this s.c. state to have the same symmetry as the s.c. ground state of the RVB ground state. This is because the nature of the interaction is the same for both states. In this case, the ground states of the NLFL and the RVB would go continuously from one to another.

Section 2. Wavefunctions

We begin with a short review of some methods in use to approach the Hubbard Hamiltonian and the introduce the trial wavefunctions for our variational approach. The Hubbard Hamiltonian had been in use implicitly [15] for some

time, when Hubbard gave it the explicit form [16a] of Eq. (1) and discussed the magnetic phase diagram by Hartree–Fock and Greens-function techniques. Furthermore [16b], he indtroduced, for the large U limit, the atomic representation (see Eq. (5)) and the operators

$$X^i_{0,0} = (1 - n_{i,\downarrow})(1 - n_{i,\uparrow})$$

$$X^i_{0,\sigma} = (1 - n_{i,-\sigma})\, c_{i,\sigma} \tag{6}$$

$$X^i_{\sigma',\sigma} = c^+_{i,\sigma'} c_{i,\sigma}(1 - n_{i,-\sigma})$$

which link the different states in the subspace of no doubly occuied site, i.e., the empty site and singly occupied site (indexed with 0 and σ, respectively). Since they do not obey fermion anticommutation rules, normal perturbation techniques are not applicable. But they form an algebra, e.g., $[X^i_{\sigma,0}, X^i_{0,\sigma'}]_+ = X^i_{\sigma,\sigma'} + \delta_{\sigma,\sigma'} X^i_{0,0}$. This property has recently been used by Ramakishnan and Shastry [17] to formulate a systematic $1/z$ expansion, where z is the number of nearest-neighbor sites, for the case of infinite U.

After Hubbard's formulation of the Hubbard Hamiltonian, Lieb and Wu [11] solved it exactly for one dimension. The resulting integral equations were evaluated numerically [18] and analytically [19]. In higher dimensions, no exact solution is known. In the limit of small U, the Hubbard model can be treated analytically by scaling theory [20].

Most approaches, mentioned so far, investigated mainly ground state properties. At high temperatures, high temperature expansions are possible [21], and normally linked to a t/U expansion. Interest [22] was concentrated mainly on the ferromagnetic T_C.

One of the most promising, in principle, exact techniques is the numerical Monte Carlo method at high but finite temperatures [23, 24]. With this method, the partition function for all small system (in two dim the size is typically between a 4×4 and an 8×8 lattice) is evaluated with use of the Trotter formula. The fermion anticommutation rules greatly increase the numerical difficulties [3].

For very small systems, exact diagonalization of the Hubbard model is possible. Since the number of states for the full Hamiltonian increases very fast, the studies have concentrated so far mainly on the case with $U = \infty$ and H_{eff} (see Refs. 25, 26], respectively). For the half-filled case, where H_{eff} reduces to the AFH Hamiltonian, Oitmaa and Betts [27] diagonalized lattices with up to 16 sites, by exploiting the full symmetry group. They find that the ground state has, in the thermodynamic limit, antiferromagnetic long range order.

Recently [28], their method to extrapolate the data to the thermodynamic limit has been questioned in view of results from spin-wave theory for small systems. Their qualitative findings, however, have been confirmed [28, 29].

1. *Variational Approach*

The approach by variational wavefunctions is complementary to that described above. The idea is to describe the ground state of the system by wavefunctions, which contain the essential physics.

We now turn to describing the wavefunctions that we consider for our approach trial wavefunctions for the ground state. Other variational wavefunctions for the half-filled case are discussed together with the presentation of the results for our approach in Section 4. We will not attempt to describe the Hubbard Hamiltonian (see Eq. (1)) directly. As discussed in Section 1.4, we will instead concentrate on H_{eff} (see Eq. (5)), which is valid in the subspace of no doubly occupied sites. In Section 1.4 we denoted wavefunctions in this subspace by $|\psi_{\text{eff}}\rangle$. We will drop in the following the subscript "eff," since we will work exclusively in the *projected subspace*, i.e., in the subspace with no doubly occupied sites.

The trial wavefunctions we consider have the general form

$$\begin{aligned} |\psi\rangle &= P_{D=0}\,|\psi_0\rangle \\ &= \prod_i (1 - n_{i,\uparrow} n_{i,\downarrow})\,|\psi_0\rangle. \end{aligned} \tag{7}$$

Here $|\psi_0\rangle$ is a simple Hartree–Fock wavefunction, $P_{D=0}$ is a projection operator, which projects on the subspace of no doubly occupied sites, and i runs over all lattice sites.

These kinds of trial wavefunctions were first proposed by Gutzwiller [30]. He considered a simple Fermi sea for $|\psi_0\rangle$. We will therefore define

$$|\text{Gutz}\rangle = P_{D=0} \prod_{\mathbf{k} \in \text{Fermi sea},\, \sigma} c^{+}_{\mathbf{k},\sigma}\,|0\rangle. \tag{8}$$

Originally [30], Gutzwiller examined a more general wavefunction, namely

$$\begin{aligned} |\psi\rangle &= P_g\,|\psi_0\rangle \\ &= \prod_i (1 - (1-g)\, n_{i,\uparrow} n_{i,\downarrow})\,|\psi_0\rangle, \end{aligned} \tag{9}$$

where $|\psi_0\rangle$ is the Fermi sea and $0 \leqslant g \leqslant 1$. For $g > 0$, this can be only a good trial wavefunction for the Hubbard Hamiltonian in the metallic region, $U < U_C$, since in this wavefunction the empty and doubly occupied sites are not bound [31]. Hence this wavefunction also has a finite conductivity in the half-filled case and will therefore not be a good trial wavefunction for the Mott insulating state. Since we are interested in describing the ground state for $U > U_C$, we will concentrate on wavefunctions of the form of Eq. (7), as trial wavefunctions for H_{eff}.

All wavefunctions $|\psi\rangle$ with no doubly occupied sites can be written in the form of Eq. (7). For a variational approach, one must specify the functional form of $|\psi_0\rangle$. The central idea for this ansatz is that it is easier to find good trial

wavefunctions for $|\psi_0\rangle$ than directly for $|\psi\rangle$. A well-defined procedure has been developed, the renormalized mean field theory, to find a functional form of $|\psi_0\rangle$. In the next two sections we briefly describe this procedure.

2. *Gutzwiller Approximative Formulas*

Gutzwiller calculated [32] the expectation value of the kinetic energy operator in $|\text{Gutz}\rangle$ in an approximate analytic way, deriving a formula now known as the *Gutzwiller approximate formula* (GAF):

$$\frac{\langle\psi|\, T\,|\psi\rangle}{\langle\psi|\psi\rangle} \approx g_t \frac{\langle\psi_0|\, T\,|\psi_0\rangle}{\langle\psi_0|\psi_0\rangle}$$
$$g_t = \frac{1-n}{1-n/2}. \tag{10}$$

Here $|\psi\rangle = P_{D=0}|\psi_0\rangle$ and T is the full kinetic energy operator of Eq. 1. Although Gutzwiller derived this formula initially for $|\psi\rangle = |\text{Gutz}\rangle$, Eq. (10) is now thought to bea good approximation formula for general $|\psi\rangle$. This formula can be derived in two ways, by simply counting the possibilities of hopping in $|\psi\rangle$ and $|\psi_0\rangle$, respectively [33], and as a two-site approximation in a systematic cluster expansion [34]. Furthermore this formula is consistent with a slave boson theory [35], which interpolates between large and small U. Note that the expectation value of the kinetic energy in $|\psi\rangle$ vanishes for $n=1$, since the hopping of the holes is the only kinetic process allowed in the projected subspace.

By the same means as that for the kinetic energy, a similar formula can be derived [36] for the n.n. spin–spin correlation:

$$\frac{\langle\psi|\, \mathbf{S}_i\cdot\mathbf{S}_j\,|\psi\rangle}{\langle\psi|\psi\rangle} \approx g_s \frac{\langle\psi_0|\, \mathbf{S}_i\cdot\mathbf{S}_j\,|\psi_0\rangle}{\langle\psi_0|\psi_0\rangle}$$
$$g_s = \frac{1}{(1-n/2)^2}. \tag{11}$$

One can test these formulas by calculating both sides of Eqs. (10) and (11) numerically. One finds [10, 36] that they work very well qualitatively; i.e., although the left and the right hand sides of Eqs. (10) and (11) might differ by about 10%, they track each other very nicely as a function of possible parameters in $|\psi\rangle$ and $|\psi_0\rangle$, respectively [36]. We describe in Section 3 the techniques employed to carry out these calculations. This analytic form for g_s (Eq. (11)) is valid only when $|\psi_0\rangle$ has no finite sublattice magnetization.

3. *Renormalized Mean Field Theory*

Here we will shortly describe the principles of renormalized mean field theory. The idea is to derive an explicit expression for $|\psi_0\rangle$ by using first the GAF formulas and then a mean field approximation for the renormalized Hamiltonian.

In a variational approach, one minimizes the expectation value of the total energy. Only in one dim [37, 38] can this expectation value be calculated without any approximations. In higher dim this must be done numerically. The idea of the renormalized mean field theory is to use the GAF formulas (Eqs. (10) and (11)) to calculate analytically the qualitative form of the best wavefunction. The numerical energy minimization is then a test and a fine tuning of these calculations. This procedure works only because the GAF formulas work qualitatively so well [36].

We rewrite H_{eff} as $T+H_s$ where $H_s=J\sum_{\langle i,j\rangle}\mathbf{S}_i\cdot\mathbf{S}_j$ (see Eq. (5)). This form is valid near half-filled to terms of order $J(1-n)$. The total energy is then given by

$$\frac{\langle\psi|\,H_{\text{eff}}\,|\psi\rangle}{\langle\psi\,|\,\psi\rangle}=\frac{\langle\psi|\,T+H_s\,|\psi\rangle}{\langle\psi\,|\,\psi\rangle}\approx\frac{\langle\psi_0|\,g_tT+g_sH_s\,|\psi_0\rangle}{\langle\psi_0|\psi_0\rangle},\tag{12}$$

where $|\psi\rangle=P_{D=0}\,|\psi_0\rangle$ and g_t and g_s are given by Eqs. (10) and (11). $g_tT+g_sH_s$ is called the renormalized Hamiltonian. The right hand side of Eq. (12) is the expectation value of the renormalized Hamiltonian in $|\psi_0\rangle$. Since $|\psi_0\rangle$ is just a standard fermionic wavefunction without any restrictions, one can use standard Hartree–Fock decoupling schemes for H_s. By this mean field approximation, the minimization of the right hand side of Eq. (12) can be done analytically [36]. In one dimension, the solution for $|\psi_0\rangle$ is just a filled Fermi sea.

4. *Projected Wavefunctions*

In two dimensions, depending on the decoupling schemes, two types of wavefunctions are obtained as solutions of the renormalized mean field theory. The choice of decoupling schemes depends on the type of order parameter introduced. The first is a projected Hartree–Fock spin density wave, $|\text{SDW}\rangle$. This solution is obtained by assuming $\langle n_{i,\uparrow}-n_{j,\downarrow}\rangle$ as order parameter in Eq. (12). Here i and j are n.n. sites,

$$|SDW\rangle=P_{D=0}\prod_{\mathbf{k}\in\text{Fermi sea},\sigma}(\tilde{u}_{\mathbf{k}}c^{+}_{\mathbf{k},\sigma}+\text{sign}(\sigma)\,\tilde{v}_{\mathbf{k}}c^{+}_{\mathbf{k}+Q,\sigma})\,|0\rangle\tag{13}$$

with

$$\tilde{u}^2_{\mathbf{k}}=\frac{1}{2}\left(1-\frac{\varepsilon_{\mathbf{k}}}{\sqrt{\varepsilon^2_{\mathbf{k}}+\Delta^2_{\text{AF}}}}\right)$$
$$\tilde{v}^2_{\mathbf{k}}=\frac{1}{2}\left(1+\frac{\varepsilon_{\mathbf{k}}}{\sqrt{\varepsilon^2_{\mathbf{k}}+\Delta^2_{\text{AF}}}}\right),\tag{14}$$

where $\varepsilon_{\mathbf{k}}$ is given by Eq. (3) and $Q=(\pi,\pi)$ for a commensurate SDW. Δ_{AF} is the antiferromagnetic order parameter.

Yokoyama and Shiba [39] have studied this wavefunction extensively. They find that it has long range antiferromagnetic order and that it yields a good description of the ground state of H_{eff} in the regime with long range antiferromagnetic order (see Fig. 4), as far as the properties of this state are known [27–29]. The properties of $|\text{SDW}\rangle$ are discussed in Section 4.

The second type of wavefunction that one can derive from renormalized mean field theory is a projected BCS wavefunction, which we will define as our RVB trial wavefunction. This solution is obtained by assuming $\langle c^+_{i,\sigma} c^+_{j,-\sigma}\rangle$ as order parameter in Eq. (12). Here i and j are n.n. sites,

$$\begin{aligned} |\text{RVB}\rangle &= P_{D=0}\,|\text{BCS}\rangle \\ &= P_{D=0}\prod_{\mathbf{k}} (u_{\mathbf{k}} + v_{\mathbf{k}} c^+_{\mathbf{k},\uparrow} c^+_{-\mathbf{k},\downarrow})\,|0\rangle. \end{aligned} \tag{15}$$

The parametrization of $u_{\mathbf{k}}$ and $v_{\mathbf{k}}$ is given by the usual BCS-form:

$$\begin{aligned} &\frac{v_{\mathbf{k}}}{u_{\mathbf{k}}} = \frac{\Delta(\mathbf{k})}{\xi_{\mathbf{k}} + \sqrt{\xi^2_{\mathbf{k}} + \Delta(\mathbf{k})^2}} =: a_{\mathbf{k}} \\ &\xi_{\mathbf{k}} = -2(\cos(k_x) + \cos(k_y)) - \mu. \end{aligned} \tag{16}$$

Here μ is a dimensionless parameter. At half filling $\mu = 0$. We discuss the meaning of μ for $n < 1$ further below. It is usual [1] to define $v_{\mathbf{k}}/u_{\mathbf{k}} =: a_{\mathbf{k}}$ as above, since this quantity will be used for the actual evaluation of $|\text{RVB}\rangle$, as we explain in Section 3. For $\Delta(\mathbf{k})$ different parametrizations are possible [40]:

$$\begin{aligned} &\Delta(\mathbf{k}) \equiv \Delta, && s\text{-wave} \\ &\Delta(\mathbf{k}) = \Delta(\cos(k_x) - \cos(k_y)), && d\text{-wave} \\ &\Delta(\mathbf{k}) = \Delta(\cos(k_x) + \cos(k_y)) - \mu, && \text{ext. } s\text{-wave}. \end{aligned} \tag{17}$$

Here Δ is the final variational parameter. In contrast to usual weak coupling BCS, the definitions for $u_{\mathbf{k}}$, and the $\Delta(\mathbf{k})$ are valid in the whole Brillouin zone and not only in a region near the Fermi surface.

It is important to note that these definitions are also valid in the half-filled case. No superconductivity can arise in a state with only singly occupied sites and $n = 1$. Hence Δ is not the true superconducting order parameter, which will be [40] proportional to $(1-n)\Delta$, as we discuss in Section 4.

From Eq. (10) we see that at half filling t drops out of Eq. (12) for the total energy, since the kinetic energy is renormalized by $(1-n)$. The only energy scale that survives renormalization for $n = 1$ is J. It would therefore be completely arbitrary to give Δ in units of t, which is a dummy variable and drops out of Eq. (16). It is more appropriate to think of Δ being dimensionless, indicating the fraction of the Brillouin zone involved in the pairing. If $\Delta \sim 1$, then $u_{\mathbf{k}} v_{\mathbf{k}}$ differs from zero in the whole Brillouin zone, whereas $u_{\mathbf{k}} v_{\mathbf{k}} \to 0$, for $\Delta \to 0$. In the latter case the

fraction of the Brillouin zone involved in the pairing goes to zero. The $\xi_{\mathbf{k}}$ that appears in the definition of $u_{\mathbf{k}}$ and $v_{\mathbf{k}}$ in Eq. (16) has the same functional form as the kinetic energy (Eq. (3)). H_s is derived by second order perturbation in T_{mix} (see Section 1.2) and is therefore, roughly speaking, proportional to the square of the kinetic energy. In renormalized mean field theory this product is then factored again.

Off half filling, the kinetic energy contributes to the total energy with a term proportional to $(1-n)t$. In renormalized mean field theory [36], this adds to $\xi_{\mathbf{k}}$ the term $-(1-n)(t/J)(\cos(k_x)+\cos(k_y))$ and therefore changes the optimal value of Δ. These changes do not introduce new qualitative features in the parametrization of $u_{\mathbf{k}}$ and $v_{\mathbf{k}}$. In this sense, spin correlations and kinetic process do not disturb each other in $|\text{RVB}\rangle$ as trial wavefunction for H_{eff}, but harmonize [41].

At half filling, all particle fluctuations in $|\text{RVB}\rangle$ are projected out; i.e., no states with less than one particle per site are present in $|\text{RVB}\rangle$ when $n=1$. That is because otherwise one could not have a mean value of one particle per site, since the projection operator projects out all states with more than one particle per site.

As defined by Eq. (16), μ is just a dimensionless variational parameter. One possible use of μ is to fix the particle number in $|\text{RVB}\rangle$, as done by Yokoyama and Shiba [42]. In this case μt takes large positive values near half filling and approaches the Fermi energy of the noninteracting system at large doping. In our calculations, we set μt equal to the Fermi energy at all fillings and work with a wavefunction which has fixed particle number N. This wavefunction is just the projection of $|\text{RVB}\rangle$ onto the subspace with particle number N: $|N\rangle = P_N|\text{RVB}\rangle$, where P_N is the corresponding projection operator. In the thermodynamic limit, it is equivalent, to work with $|\text{RVB}\rangle$ or with $|N\rangle$, if N corresponds to the mean number of particles in $|\text{RVB}\rangle$. For computational reasons, we will work mainly with $|N\rangle$. For the rest of this paper, we will denote by $|\text{RVB}\rangle$ both $|N\rangle$ and the original $|\text{RVB}\rangle$. Whenever necessary, we will explicitly state whether this wavefunction is supposed to have a fixed number of particles or not.

We remark that other authors take different forms for $\xi_{\mathbf{k}}$ in Eq. (16) [41, 43–45]. One must therefore be very careful about terminology. What we call "*d*-wave" is at half filling [36] identical to what Kotliar [43] calls "$s+id$-wave" and what Affleck and Marston [45] call "flux state." This is due to the redundancy in a fermion representation of spin wavefunctions [36].

5. *Why Projected Wavefunctions?*

We are now in the position to recapitulate the two central steps in the approach by projected wavefunctions.

1. Transformation of the Hilbert space as described in Section 1.2. This transformation eliminates processes which change the total number of doubly occupied sites. Since we are interested only in low energy processes, we approximate the transformed Hamiltonian, H_{eff}, by Eq. (5). This corresponds to an expansion in t/U. This Hamiltonian has matrix elements only in the subspace with no doubly

occupied sites. In this way we assure that we describe a Mott insulating state in the half-filled case. Without this transformation, it is difficult to describe a Mott insulator variationally (see Section 1.4).

2. As a variational ansatz for the trial wavefunction we take $|\psi\rangle = P_{D=0}|\psi_0\rangle$ (see Eq. (7)). This ansatz has two merits. A direct variational ansatz for $|\psi\rangle$ is difficult. A straightforward and physically transparent procedure has been developed to find a analytical form for $|\psi_0\rangle$. This is achieved by the renormalized renormalized mean field theory (see Section 2.4). The wavefunction, $|\psi\rangle$, derived in this way, has only a few variational parameters. This property is very important for the numerical evaluation. The second merit of this ansatz is the fermion representation. $|\psi\rangle$ is explicitly written in terms of fermion creation operators. No problem with antisymmetrization arises and the properties of projected wavefunctions can be calculated with the same ease for both finite doping and the half-filled case.

Section 3. Methods

1. *Monte Carlo Procedure*

We now outline the method we use to evaluate numerically the projected wavefunctions. Only in one dimension [37, 38] we know the properties of the Gutzwiller wavefunction analytically. In higher dimensions and for general projected wavefunctions, we must resort to numerical methods.

Our problem is to evaluate expectation values of an operator Θ in $|\psi\rangle$ for a finite system:

$$\langle\Theta\rangle = \frac{\langle\psi|\,\Theta\,|\psi\rangle}{\langle\psi|\psi\rangle} = \sum_{\alpha,\beta}\langle\alpha|\,\Theta\,|\beta\rangle\frac{\langle\psi|\alpha\rangle\langle\beta|\psi\rangle}{\langle\psi|\psi\rangle}. \tag{18}$$

Here, α, β are states in which the electron spins have definite spatial configurations. In other words, α is a label specifying the two disjoint sets $\{R_1 \cdots R_{N_\uparrow}\}$ and $\{R'_1 \cdots R'_{N_\downarrow}\}$ which determines the positions of the up- and down-spin electrons, respectively. In terms of fermion creation operators,

$$|\alpha\rangle = c^+_{R_1,\uparrow}\cdots c^+_{R_{N_\uparrow},\uparrow}c^+_{R'_1,\downarrow}\cdots c^+_{R'_{N_\downarrow},\downarrow}|0\rangle.$$

The specific form of $\langle\alpha|\psi\rangle$ depends on $|\psi\rangle$ (see Sections 3.2 and 3.3).

Horsch and Kaplan [46] recognized that this sort of expectation value is susceptible to a Monte Carlo (MC) evaluation. They applied it to the half-filled case and Shiba [47] has implemented this method for the two band infinite U Gutzwiller wavefunction for the periodic Anderson model.

We rewrite Eq. (18) as

$$\langle \Theta \rangle = \sum_{\alpha} \left(\sum_{\beta} \frac{\langle \alpha | \Theta | \beta \rangle \langle \beta | \psi \rangle}{\langle \alpha | \psi \rangle} \right) \frac{|\langle \alpha | \psi \rangle|^2}{\langle \psi | \psi \rangle}$$
$$= \sum_{\alpha} f(\alpha)\, \rho(\alpha), \tag{19}$$

with

$$f(\alpha) = \sum_{\beta} \frac{\langle \alpha | \Theta | \beta \rangle \langle \beta | \psi \rangle}{\langle \alpha | \psi \rangle}$$
$$\rho(\alpha) = \frac{|\langle \alpha | \psi \rangle|^2}{\langle \psi | \psi \rangle}. \tag{20}$$

It follows that

$$\rho(\alpha) \geqslant 0, \qquad \sum_{\alpha} \rho(\alpha) = 1. \tag{21}$$

Therefore, $\langle \Theta \rangle$ can be evaluated by a random walk through configuration space with weight $\rho(\alpha)$. The MC weighting factor $T(\alpha \to \alpha')$ for going from one configuration α to another configuration α' can be chosen as

$$T(\alpha \to \alpha') = \begin{cases} 1, & \rho(\alpha') > \rho(\alpha) \\ \rho(\alpha')/\rho(\alpha), & \rho(\alpha') < \rho(\alpha). \end{cases} \tag{22}$$

The configuration α' is accepted with probability $T(\alpha \to \alpha')$.

We will use α', which are generated from α by the interchange of two electrons with opposite spin or by the motion of an electron to an empty site. By this choice of α' the time needed to compute $T(\alpha \to \alpha')$ is cut down drastically with respect to a random choice of α' (see Section 3.4).

It is possible to restrict the possible α' to those configurations, which can be generated out of α by the interchange of n.n. electrons of opposite spins only [46] or by the motion of an electron to a n.n. empty site. In this case, the MC weighting factors are multiplied by a configurational weighting factor, which is given by the ratio of possible new configurations in α' and α, respectively [46]. The so-constructed random walks are still ergodic, but the acceptance rate, i.e., the average of $T(\alpha \to \alpha')$, is enhanced. This is advantageous, since the computation of $T(\alpha \to \alpha')$ is expensive.

By this procedure, a series of configurations $\{\alpha_1, \alpha_2, ..., \alpha_{N_{MC}}\}$ is generated, where N_{MC} is the total number of MC steps. $\langle \Theta \rangle$ is given by

$$\langle \Theta \rangle = \frac{1}{N_{MC}} \sum_{i=1}^{N_{MC}} f(\alpha_i). \tag{23}$$

Since the α_i's are not statistically independent, it is possible to replace the sum in Eq. (23) by a sum over a subset $\{\tilde{\alpha}_j\}$ of $\{\alpha_i\}$, without losing accuracy. For example, one can make a measurement $f(\tilde{\alpha}_j)$ only after every Lth MC-updating, where L is the total number of lattice sites. This may accelerate the calculation, whenever the computation of $f(\alpha)$ is time expensive. In this case, the expectation value for Θ is given by $\langle\Theta\rangle = \tilde{N}_{\mathrm{MC}}^{-1} \sum_j f(\tilde{\alpha}_j)$, where $\tilde{N}_{\mathrm{MC}}$ is the number of measurements. It is not advantageous to perform measurements at still larger intervals, since the $\{\tilde{\alpha}_j\}$ are already nearly statistically independent, when we take for $\tilde{\alpha}_j$ every Lth α_i.

The amount of computation time needed to calculate $f(\alpha)$ depends mainly on the number of spin configurations β with nonvanishing matrix elements $\langle\beta|\,\Theta\,|\alpha\rangle$ (see Eq. (20)). For operators Θ diagonal in α, e.g., the z-component of the spin–spin interaction energy, $\sum_{\langle i,j\rangle} S_i^z S_j^z$, there is only one $\beta = \alpha$.

For the kinetic energy operator, there are about $z \cdot N_h$ configurations β, where z is the number of n.n. sites and N_h the number of empty sites. For the xy-component of the spin–spin interaction energy, namely $\sum_{\langle i,j\rangle} \frac{1}{2}(S_i^+ S_j^- + S_i^- S_j^+)$, the number of configurations β is of the order of L. For the calculation of this quantity, it is therefore important to use only the $\tilde{\alpha}_j$ for the expectation value in Eq. (23) and not each α_i.

The total number of MC steps is normally much lower than the total number of spin configurations. It is therefore necessary to estimate the accuracy of $\langle\Theta\rangle$ as calculated by Eq. (23). This is done by doing N_r independent MC runs ($N_r \sim 10$), with different random initial spin configurations. In this way, one obtains N_r independent $\langle\Theta\rangle_l$, where each $\langle\Theta\rangle_l$ is the average of a large number of measurements $f(\tilde{\alpha}_j)$. The expectation value of Θ in $|\psi\rangle$ is then defined by the average

$$\overline{\langle\Theta\rangle} = \frac{1}{N_r} \sum_{l=1}^{N_r} \langle\Theta\rangle_l. \tag{24}$$

The accuracy is then given by the standard deviation

$$\sqrt{\frac{1}{(N_r - 1)} \sum_{l=1}^{N_r} (\langle\Theta\rangle_l - \overline{\langle\Theta\rangle})^2}. \tag{25}$$

The measurement of the error bars by Eq. (25) is very reliable in the following sense: Data from repeated calculations for the same system with different random initial spin configurations scatter with a distribution given by Eq. (25). Further, we do not expect corrections due to systematic errors. No source of possible systematic errors is known for this type of calculation. The estimate of the accuracy by Eq. (25) is valid for a definite lattice size and particle number. The estimation of accuracy of results extrapolated to the thermodynamic limit is more complicated and is discussed in Section 3.5.

2. *Amplitudes for the Spin Density Wave*

The key quantity for the MC calculations described in the previous section, are the amplitudes of the trial wavefunction in a given spin configuration: $\langle \alpha | \psi \rangle$. It is necessary to know their form and an efficient way to calculate them.

For an equal number of up- and down-spins, N_σ, $\langle \alpha | \psi \rangle$ is the determinant of an $N_\sigma \times N_\sigma$ matrix A_α. More generally, for an arbitrary number of down- and up-spins $(N_\downarrow, N_\uparrow)$ and for $|\psi\rangle = |\text{Gutz}\rangle$ or $|\psi\rangle = |\text{SDW}\rangle$, $\langle \alpha | \psi \rangle$ is the product of the determinant of an $N_\downarrow \times N_\downarrow$ matrix $(A_{\alpha,\downarrow})$ and the determinant of an $N_\uparrow \times N_\uparrow$ matrix $(A_{\alpha,\uparrow})$. The (j, l)th element of these matrices is given by (see Eq. (13) $\tilde{u}_{\mathbf{k}_j} \exp(i\mathbf{k}_j \cdot \mathbf{R}_{l,\sigma}) + \text{sign}(\sigma)\, \tilde{v}_{\mathbf{k}_j} \exp(i(\mathbf{k}+\mathbf{Q}) \cdot \mathbf{R}_{l,\sigma})$. Here $\{\mathbf{k}_j\}$ is the set of $\mathbf{k}$-vectors which form the σ Fermi sea and $\{\mathbf{R}_{l,\sigma}\}$ denotes the position of the σ-spins. For the Gutzwiller state, $\tilde{u}_\mathbf{k} \equiv 1$ and $\tilde{v}_\mathbf{k} \equiv 0$.

For an equal number of down- and up-spins, $N_\downarrow = N_\uparrow = N/2$, the two determinants can be combined into a determinant of a single matrix A_α, by multiplication of the corresponding matrices. We can see this in the following way: We assume $\tilde{u}_\mathbf{k} = \tilde{u}_{-\mathbf{k}}$, $\tilde{v}_\mathbf{k} = \tilde{v}_{-\mathbf{k}}$ and define

$$\begin{aligned} a_\mathbf{k}(\mathbf{R}_{j,\downarrow}) &= \tilde{u}_\mathbf{k} \exp(i\mathbf{k} \cdot \mathbf{R}_{j,\downarrow}) - \tilde{v}_\mathbf{k} \exp(i(\mathbf{k}+\mathbf{Q}) \cdot \mathbf{R}_{j,\downarrow}) \\ a_\mathbf{k}(\mathbf{R}_{l,\uparrow}) &= \tilde{u}_\mathbf{k} \exp(i\mathbf{k} \cdot \mathbf{R}_{l,\uparrow}) + \tilde{v}_\mathbf{k} \exp(i(\mathbf{k}+\mathbf{Q}) \cdot \mathbf{R}_{l,\uparrow}) \\ a(\mathbf{R}_{j,\downarrow}, \mathbf{R}_{l,\uparrow}) &= \sum_{\mathbf{k} \in \text{Fermi sea}} a_\mathbf{k}(\mathbf{R}_{l,\uparrow})\, a_{-\mathbf{k}}(\mathbf{R}_{j,\downarrow}). \end{aligned} \tag{26}$$

Because of the cross terms, $\sim \tilde{u}_\mathbf{k} \tilde{v}_\mathbf{k}$, $a(\mathbf{R}_{j,\downarrow}, \mathbf{R}_{l,\uparrow})$ is not a function of $\mathbf{r} = \mathbf{R}_{j,\downarrow} - \mathbf{R}_{l,\uparrow}$ alone. With the help of these definitions, we rewrite Eq. (13) as

$$\begin{aligned} |\text{SDW}\rangle &= P_{D=0} \prod_{\mathbf{k} \in \text{Fermi sea}} \sum_{\mathbf{R}_{j,\downarrow},\, \mathbf{R}_{l,\uparrow}} a_\mathbf{k}(\mathbf{R}_{l,\uparrow})\, a_{-\mathbf{k}}(\mathbf{R}_{j,\downarrow})\, c^+_{\mathbf{R}_{l,\uparrow},\uparrow} c^+_{\mathbf{R}_{j,\downarrow},\downarrow} |0\rangle \\ &= P_{D=0} \left(\sum_{\mathbf{R}_{j,\downarrow},\, \mathbf{R}_{i,\uparrow}} a(\mathbf{R}_{j,\downarrow}, \mathbf{R}_{l,\uparrow})\, c^+_{\mathbf{R}_{l,\uparrow},\uparrow} c^+_{\mathbf{R}_{j,\downarrow},\downarrow} \right)^{N/2} |0\rangle \\ &= \sum_\alpha \langle \alpha | \text{SDW} \rangle\, |\alpha\rangle. \end{aligned} \tag{27}$$

This equality would be true also without the projection operator $P_{D=0}$. The amplitude, $\langle \alpha | \text{SDW} \rangle$, is given [40, 48] by the determinant of A_α, which has the form

$$\begin{pmatrix} a(\mathbf{R}_{1,\downarrow}, \mathbf{R}_{1,\uparrow}) & a(\mathbf{R}_{1,\downarrow}, \mathbf{R}_{2,\uparrow}) & \cdots & a(\mathbf{R}_{1,\downarrow}, \mathbf{R}_{N_\sigma,\uparrow}) \\ a(\mathbf{R}_{2,\downarrow}, \mathbf{R}_{1,\uparrow}) & a(\mathbf{R}_{2,\downarrow}, \mathbf{R}_{2,\uparrow}) & & a(\mathbf{R}_{2,\downarrow}, \mathbf{R}_{N_\sigma,\uparrow}) \\ \vdots & & \ddots & \vdots \\ a(\mathbf{R}_{N_\sigma,\downarrow}, \mathbf{R}_{1,\uparrow}) & a(\mathbf{R}_{N_\sigma,\downarrow}, \mathbf{R}_{2,\uparrow}) & \cdots & a(\mathbf{R}_{N_\sigma,\downarrow}, \mathbf{R}_{N_\sigma,\uparrow}) \end{pmatrix}. \tag{28}$$

To derive this, we must expand Eq. (27) and gather all terms which contribute to the same spin configuration α. The number and functional form of these terms are obviously the same as those for $|A_\alpha|$. Then we must order these terms in two steps: First we anticommute all up-spin creation operators to the left. By this we do not change the relative sign of the different terms. Second, we order the up- and down-spin creation operators separately, but in the same way for all terms. Their relative sign is then determined by the fermion anticommutation rules. These anticommutation rules are obviously reproduced by the determinal form.

3. *Amplitudes for the Resonating Valence Bond State*

The amplitudes $\langle \alpha | \mathrm{RVB} \rangle$ can be written in the form of Eq. (28), with a different form for $a(\mathbf{R}_{j,\downarrow}, \mathbf{R}_{l,\uparrow})$. To see this, we follow Anderson [1] and define $a(\mathbf{r})$ as the Fourier transform of $a_\mathbf{k} = v_\mathbf{k}/u_\mathbf{k}$ (see Eq. (16)). Here $\mathbf{r} = \mathbf{R}_{j,\downarrow} - \mathbf{R}_{l,\uparrow}$,

$$a(\mathbf{r}) = \sum_\mathbf{k} a_\mathbf{k} \cos(\mathbf{k} \cdot \mathbf{r}). \tag{29}$$

This form is valid, if $a_\mathbf{k} = a_{-\mathbf{k}}$.

In the $\mathbf{k}$-summation of Eq. (29), the term $\mathbf{k} = 0$ is not well defined for the d-wave (see Eq. (17)), since $a_{\mathbf{k}=0}$ is a fraction where both the numerator and the denominator are zero. From numerical calculations we have found that $a_{\mathbf{k}=0}$ must be large, in order to have a good spin–spin interaction energy. This is confirmed by exact diagonalization of small clusters [49], which give the result that the best RVB-state at half filling is the d-wave with $a_{\mathbf{k}=0} = \infty$. This means that the $\mathbf{k} = 0$ state is occupied by both a down- and an up-spin electron. In our calculations, we have generally taken $a_{\mathbf{k}=0} = \sqrt{L}$. This form for $a_{\mathbf{k}=0}$ yields the correct limiting behaviour for large systems, but for a small number of sites the state so defined is high in energy. The limiting value for $a_{\mathbf{k}=0}$ for the lowest d-wave RVB state for $L = 10$ is much larger.

The RVB wavefunction, as defined by Eq. (15), is a superposition of states with different particle numbers, except at half filling (see Section 2.4). Yokoyama and Shiba [42] have developed a method especially appropriate to evaluate numerically this wavefunction.

Here we will concentrate on the projection of $|\mathrm{RVB}\rangle$ on the subspace with fixed number of particles $N = 2 \cdot N_\sigma$: $|N\rangle = P_N |\mathrm{RVB}\rangle$ (see Section 2.4). With the use of Eq. (29), we write [1] $|N\rangle$ as

$$\begin{aligned} |N\rangle &= P_N P_{D=0} \prod_\mathbf{k} (u_\mathbf{k} + v_\mathbf{k} c^+_{\mathbf{k},\uparrow} c^+_{-\mathbf{k},\downarrow}) |0\rangle \\ &= P_{D=0} \left(\sum_{\mathbf{R}_{j,\downarrow}, \mathbf{R}_{l,\uparrow}} a(\mathbf{R}_{j,\downarrow} - \mathbf{R}_{l,\uparrow}) c^+_{\mathbf{R}_{l,\uparrow},\uparrow} c^+_{\mathbf{R}_{j,\downarrow},\downarrow} \right)^{N/2} |0\rangle. \end{aligned} \tag{30}$$

As for the case of the SDW, $\langle \alpha | N \rangle$ is a determinant of an $N_\sigma \times N_\sigma$ matrix (see Eq. (26)) with elements $a(\mathbf{R}_{j,\downarrow} - \mathbf{R}_{l,\uparrow})$ where $a(\Delta\mathbf{R})$ is given by Eq. (29). Note that translation invariance is not broken, in contrast to the SDW-case.

4. *Calculation of the Determinants*

In the preceding sections we showed that the amplitudes of projected wavefunctions have the form of $N/2 \times N/2$ determinants. In the MC process for the calculation of $\langle \Theta \rangle$, the whole series $|A_{\alpha_1}|$, $|A_{\alpha_2}|$, ..., $|A_{\alpha_{N_{MC}}}|$ must be calculated. Two problems arise: First it is necessary to calculate determinants, or the ration of the determinants in an efficient way. Second, for nondiagonal operators Θ, one must keep track of the relative sign of the determinants.

The second issue can be handled in the following way: The initial ordering of the fermion creation operators is chosen randomly: $|\alpha\rangle = c^+_{R_{1,\uparrow}} c^+_{R_{2,\uparrow}} \cdots c^+_{R_{N_\uparrow,\uparrow}} c^+_{R'_{1,\downarrow}} \cdots c^+_{R'_{N_\downarrow,\downarrow}} |0\rangle$. Then $\langle \alpha | \psi \rangle = |A_\alpha|$, where A_α is given by Eq. (28). Let us consider now $\langle \hat{\alpha} | \psi \rangle$, where $\hat{\alpha}$ differs from α only by the motion of the second up-spin to a new site: $|\hat{\alpha}\rangle = c^+_{R_{1,\uparrow}} c^+_{\hat{R}_{2,\uparrow}} \cdots c^+_{R_{N_\uparrow},\uparrow} c^+_{R'_{1,\downarrow}} \cdots c^+_{R'_{N_\downarrow,\downarrow}} |0\rangle$. Such amplitudes are needed for the calculation of the expectation value of the kinetic energy; the matrix element $\langle \tilde{\alpha} | T | \alpha \rangle$ does not vanish. The new amplitude is given now by the determinant of $A_{\tilde{\alpha}}$, which differs from A_α only by the substitution of R_2 by $\hat{R}_2$ in the second column. For this to be true, one must express Θ in terms of fermion creation operators and to order them in a way that is consistent with the ordering described above. For the kinetic energy, this is naturally the case. The xy-component of the spin–spin interaction becomes $S^+_i \cdot S^-_j = c^+_{i,\uparrow} c_{i,\downarrow} c^+_{j,\downarrow} c_{j,\uparrow} = -c^+_{i,\uparrow} c_{j,\uparrow} c^+_{j,\downarrow} c_{i,\downarrow}$. In this case, both a column and a row in Eq. (28) are replaced as described above, for the new amplitude.

The key quantity for the MC evaluation of the projected wavefunctions is the ratio of two determinants, $|A_{\alpha'}|/|A_\alpha|$, where the two spin configurations α and α' differ by the interchange of two electrons with opposite spin, or by the interchange of an electron and an empty site (see Eqs. (20), (22), and (28)).

The number of computation steps necessary to compute a single determinant of an $N_\sigma \times N_\sigma$ matrix is proportional to N^3_σ. For the above problem, a more efficient algorithm exists, which involves only $\sim N^2_\sigma$ computation steps. This algorithm was first introduced by Ceperly *et al.* [50] for the MC evaluation of fermionic trial wavefunctions.

The trick is to store not only the matrix A_α but also its inverse, A^{-1}_α. In each MC step, whenever a new configuration α' is accepted, not only A_α is updated but also A^{-1}_α. For this, only $\sim N^2_\sigma$ computation steps are needed. The same number of computation steps is also needed to calculate the ratio of he two determinants, by using the inverse of one of them ($|A_{\alpha'}|/|A_\alpha| = |A_{\alpha'} A^{-1}_\alpha|$). This procedure works only because α' is chosen to differ from α only by the interchange of two electrons with opposite spins or by the interchange of an electron and an empty site. In this case A_α and $A_{\alpha'}$ differ only by one row and one column.

In one dimension, it is possible to calculate the ratio of determinants in a still more efficient way, for the projected Fermi sea. In this case, the determinants have the form of a Vandermonde determinant [10], which can be factorized. The total number of steps to calculate the ratio of two determinants is then only proportional to N_σ.

5. *Extrapolation to the Thermodynamic Limit*

A correct extrapolation to the thermodynamic limit is essential in order to describe the properties of the wavefunctions reliably. One is faced with similar problems for the results obtained by exact diagonalization of H_{eff} for small clusters. In this case, the extrapolation can be done only at half filling. To see this, just note that 10% doping means one hole in 10 sites and two holes in a 20-site system. The later diagonalization problem is beyond the computational power of present computer generations.

In order to obtain a smooth extrapolation of the data to the thermodynamic limit, we use lattices with a total number of sites [27, 51] $L=(2n+1)^2+1=$ 10, 26, 50, 82, 122, 170, 226, ... and periodic boundary conditions (n is an integer). In Fig. 5 the case $L=26$ is illustrated.

This set of lattices has the property that at half filling the projected Fermi sea is nondegenerate. All shells of **k**-vectors are completely filled or empty. At finite doping, this is the case if we use only hole concentrations, where the total number of holes is a multiple of eight. This property assures a smooth extrapolation to the thermodynamic limit [51]. For other kinds of lattices, the Fermi surface is not uniquely defined. Several nonoccupied **k**-states lie on the Fermi surface. As a consequence, the behaviour of the projected wavefunctions is not monotonic as a function of L. Oscillations in the expectation value of the energy occur. Extrapolation to the thermodynamic limit is therefore more difficult.

In addition, these lattices have the convenient property that only two **k**-vectors lie on the diagonals, namely $(0, 0)$ and (π, π). This is convenient for the calculation of the d-wave $|\text{RVB}\rangle$, for which $a(\mathbf{k})$ is not well defined on the diagonals (see Section 3.3).

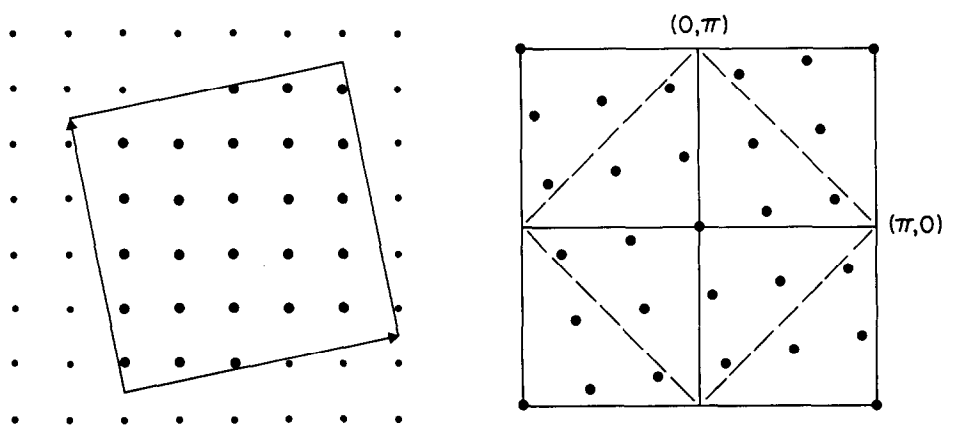

FIG. 5. Illustration of the type of lattices used for the Monte Carlo calculations for 26 sites. (Left) The lattice in real space. The sites are given by the bold dots inside the square. The arrows indicate the periodic boundary conditions. (Right) The lattice in momentum space. The dots are the values of the **k**-vectors. Note that the Fermi sea at half filling, given by the dots inside the dashed square, contains 13 **k**-states, the number of down- or up-spins. Note that the four **k**-vectors $(\pm\pi, \pm\pi)$ are equivalent.

An alternative set of lattices, which ensures the same properties as described above, has been employed by Yokoyama and Shiba [42]. These are 4×4, 6×6, ... lattices, with periodic and antiperiodic boundary conditions in x- and y-directions, respectively.

Obviously, an extrapolation with a constant density of holes cannot be done, except for $n = 1$. We therefore prefer to work with a fixed number of holes and to renormalize the measured quantity by a function of $(1-n)$. Within this approach, the extrapolation $L \to \infty$ implies $(1-n) \to 0$. In this limit, the calculations of the properties of the projected wavefunctions are most reliable.

For a reliable extrapolation of the data to the thermodynamic limit, a knowledge of the qualitative behaviour of the finite size corrections on $1/L$ is necessary. This is not known for the projected wavefunctions. One must therefore extract this behaviour empirically from a plot of the data. By this procedure one obtains small error bars for the extrapolated results. But if the qualitative extrapolation is not correct, these error bars are meaningless.

On the other hand, the data increase or decrease often monotonically as a function of L, especially when we use lattices of the type described above. An alternative approach for the estimate of the expectation values in the thermodynamic limit is then possible. One increases the lattice size up to the point where the difference between the results of the two largest lattices is smaller than the error bars (given by Eq. (25)). A reliable estimate for the result in the thermodynamic limit is then just the expectation value and accuracy of the largest calculated lattice. By this procedure one assures that the finite size corrections are less than the error bars, although these are generally somewhat larger than those obtained by the first method.

In our calculation, we have generally employed the second method. When presenting the results of our calculations in Section 4, we explicitly state whenever the first method was used.

Section 4. Results

We now come to the presentation and discussion of results obtained by evaluation of the projected wavefunctions by the variational Monte Carlo method.

The projected wavefunction lowest in energy for H_{eff} in one dimension is the projected Fermi sea [36]. As a trial wavefunction for the Hubbard model, the more general wavefunction as defined by Eq. (9) has been studied by the MC technique [52, 53] (see the discussion following Eq. (9)). In one dimension, the properties of this wavefunction have been calculated exactly [37, 38], by the resummation of all diagrams in a perturbative expansion.

Recently, a variational wavefunction first introduced by Marshall [54] was reexamined by a variational MC technique [55, 56]. Since this wavefunction exhibits a finite staggered magnetization even in one dimension [55], the physical

relevance of the Marshall wavefunction for this case is not clear. We therefore postpone discussion of them to Section 4.3.

For the one-dimensional case, another trial wavefunction, based on triplet excitations of a valence bond state, has been proposed recently [57] in the context of high T_C superconductivity.

1. *One Dimension—Half Filling*

We now turn to discussion of the Gutzwiller wavefunction in one dimension, for the half-filled case. We will discuss only the properties of $|\text{Gutz}\rangle$. Both the $|\text{RVB}\rangle$ and the $|\text{SDW}\rangle$ are higher in energy [36, 39]. This means that the additional variational degrees of freedom, present in these two kinds of wavefunctions, are physically not relevant in one dimension. Within the framework of projected wavefunctions, $|\text{Gutz}\rangle$ is therefore stable against the introduction of both antiferromagnetic and superconducting correlations.

A consensus has been reached that $|\text{Gutz}\rangle$ is an excellent trial wavefunction for the ground state of the one-dim. Heisenberg model. The energy for $|\text{Gutz}\rangle$ differs only by 0.2% from the exact ground state energy [10, 38]. Furthermore [38, 46], the spin–spin correlations fall off with the distance j like $(-1)^j/j$, as they do for the exact solution [58]. Clearly, no long range antiferromagnetic order is present, since it is quenched by the low dimensionality [12].

The Gutzwiller wavefunction is intimately related with short range antiferromagnetism in one dimension. This is shown by the work of Shastry [59] and Haldane [60], who showed that $|\text{Gutz}\rangle$ is the exact ground state of an antiferromagnetic Heisenberg chain, with couplings, that fall off with the distance j as $1/j^2$.

It is possible to describe excited states by creating particle–hole excitation in $|\psi_0\rangle$. The exact relation between the projection of these excited states of $|\psi_0\rangle$ and the excitation of H_{eff} is unclear, since the set of all projected wavefunctions is overcomplete in the projected subspace. The number of states in the full Hilbert space is $\binom{N_\downarrow}{L}\binom{N_\uparrow}{L}$, while the number of states in the projected space, $\binom{N_\sigma}{L}$ at half filling, is much lower. Every state in the original Hilbert space can be projected; the number of projected wavefunctions is therefore vastly overcomplete. Attempts have been made to relate the lowest projected particle–hole excitations of $|\psi_0\rangle$ at half filling [61] with the Des Cloiseaux–Pearson [62] spectrum.

Within the set of projected wavefunctions having a fixed magnetisation $m = (N_\uparrow - N_\downarrow)/(N_\uparrow + N_\downarrow)$, the state lowest in energy is given by

$$|\text{Gutz}(m)\rangle = P_{D=0} \prod_{|k| \leq k_{F,\uparrow}} c^+_{k,\uparrow} \prod_{|k| \leq k_{F,\downarrow}} c^+_{k,\downarrow} |0\rangle, \tag{31}$$

where $k_{F,\sigma} = \pi(N_\sigma - 1)/L$. N_σ must be odd for $|\text{Gutz}(m)\rangle$ to be well defined.

Using this trial wavefunction, the spin susceptibility can be calculated [10]. It is found to be close to the susceptibility of the exact solution [63]. The results are given in Table I.

TABLE I

Results for One Dimension

	$\langle \mathbf{S}_i \cdot \mathbf{S}_j \rangle$	χ	$\langle T \rangle$
Gutzwiller	$-0.442\,118$ [38]	0.058 ± 0.008 [10]	$-1.887 \pm 0.05\,t$
Exact for H_{eff}	$-0.443\,147$ [11]	0.0506 [63]	$-2.0\,t$ [18]

Note. The first and second columns show for half filling the nearest-neighbor spin–spin correlation energy in units of $J = 4t^2/U$ and the spin susceptibility in units of $2g^2\mu_B^2/J$, respectively. The third column shows the kinetic energy per hole, in the limit of vanishing hole density. The first row shows the results of the above quantities for the projected Fermi sea, the Gutzwiller wavefunction, while the second row shows the values for the exact ground state of H_{eff}. The numbers in brackets indicate the reference from which the entry is taken.

2. *Nearly Localized Fermi Liquid*

At finite doping, we will consider the case when the density f holes is small compared with unity, but large enough so that the excitations can be described by quasi-particle excitations of a Fermi liquid.

This is the case when $t/U \ll 2(1-n)$, as discussed in Section 1.5. In this limit, only the projected kinetic energy operator survives in the expression for H_{eff} in Eq. (5). H_{eff} describes then a "nearly localized Fermi liquid" (NLFL). Note that within this one band model, we will not describe a NLFL in the limit $(1-n) \to 0$, at constant ratio t/U, since in this limit the spin-wave excitations dominate.

The contribution of the kinetic energy to the ground state energy is shown in Table I. We see that the value for the Gutzwiller wavefunction is quite close to that for the exact ground state of H_{eff}. For the exact ground state [18], the bandwidth of the holes, for low hole concentrations, is the bare bandwidth $4t$, as it is for infinite U for all hole concentrations [10]. This is particular to one dimension, since the fermions cannot cross.

Although the n.n. spin–spin correlations do not contribute substantially to the total ground state energy of H_{eff} in this parameter region, they are very strong. They are therefore not dynamical in nature, i.e., due to the spin interaction term in the Hamiltonian, but a consequence of the strong on-site Coulomb repulsion. The minimization of the kinetic energy of the holes and the exclusion of doubly occupied sites enforce the spin–spin correlations [10].

The contribution of the spin–spin correlations to the total ground state energy is not large, for $t/U \ll 2(1-n)$, but essential in two and three dimensions to stabilize the NLFL against the ferromagnetic instability (see Section 1.3). The ferromagnetic phase is stable for $t/U \to 0$ in two and three dimensions. In one dim all spin configurations are degenerate, for $U = \infty$, since the fermions cannot cross [10]. It is not correct to deduce from these facts that the NLFL is nearly ferromagnetic. In our approach by projected wavefunctions, the NLFL is almost localized and therefore nearly antiferromagnetic. The transition to the ferromagnetic phase, as a

functions of t/U, at constant $(1-n)$, should be of first order. This is because the strong antiferromagnetic short ranged spin–spin correlations are present wherever the NLFL is stable, since they are not consequence of the dynamics, but of the strong on-site Coulomb repulsion.

It is important to note that the strong short ranged spin–spin correlations are present only at low temperatures [10]. The temperature scale at which they disappear is the energy scale of the excitations in $|\psi\rangle$, which is $\sim(1-n)t$. This is normally expressed by saying that the Fermi temperature is renormalized by $(1-n)$: $T_F^* = (1-n)T_F$. This energy renormalization is valid only in the Fermi liquid regime, i.e., for $|\text{Gutz}\rangle$, and not for a more general projected wavefunction like $|\text{SDW}\rangle$ or $|\text{RVB}\rangle$. We will now shortly discuss the mechanism for this energy renormalization for the Fermi liquid wavefunction.

We must be careful about the term "Fermi liquid" in one dimension. Quasi-particles are not defined, since their lifetime remains constant in the limit of vanishing temperature. In one dim we examine the energy of the particle–hole excitations. We expect that the generalization of $|\text{Gutz}\rangle$ and of the excited states to three dim will show the same qualitative behaviour. The excitations correspond then to well-defined quasi-particles.

For $t/U \ll 2(1-n)$, only the projected kinetic energy survives in the expression for H_{eff} as described by Eq. (5). The spin degrees of freedom are disordered by the motion of the holes, which have a bandwidth $\sim t$. In a system of interacting fermions, the volume of the Fermi surface is unchanged [64] with respect to the noninteracting case, if the system can still be described by Fermi liquid theory. The excitations are therefore quasi-particles, in a one to one correspondence with the excitations of the noninteracting system. These quasi-particles have an enhanced effective mass $m^* = m/(1-n)$. The disordering of the spin degree of freedom gives rise to an entropy of $R \cdot \ln(2)$ at a temperature scale of T_F^*, which yields consequently a very large specific heat [65], which, in three dim, would be linear in temperature. In a one band picture, this physics has been worked out in a phenomenological model for the heavy electron systems [66] and for normal liquid ^{3}He [67].

3. *Two Dimensions—Other Variational Approaches*

The field of variational approaches to H_{eff} is in rapid development. No final review can be given here even for the projected wavefunctions, but very interesting results are already available.

Apart from the projected wavefunctions, two alternative wavefunctions have been studied recently in two dimensions at half filling. Both are formulated in terms of spin operators and not in terms of fermion creation operators, as the projected wavefunctions. Therefore, they are not readily generalized to finite doping.

The first has been formulated by Marshall [54] an recently reexamined by Huse and Elser [55] and by Horsch and von der Linden [56]. The second ones are RVB-type wavefunctions, considered by Liang, Doucot, and Anderson [69]

(LDA), which are formulated as a superposition of singlet-bond configurations in real space. Both classes of wavefunctions satisfy explicitly Marshall's criterion [54].

This criterion determines the sign of the amplitude of a given spin configuration of the ground state of the antiferromagnetic Heisenberg model. This sign is $+1$ if an even number of σ-spins is on one of the two sublattices and -1 otherwise. It seems to be important for a trial wavefunction to satisfy this criterion, in order to have a very good energy.

The Marshall wavefunction yields a very low energy (see Table II) and serves therefore as a benchmark for both of the other variational approaches and for correct extrapolation of results obtained by exact diagonalization of small clusters [27, 28]. This wavefunction shows long range antiferromagnetic order, with moments ordered in the xy-plane. The ordered moment has $\sim 71\%$ of its classical value [55].

The LDA wavefunctions have many more variational degrees of freedom. They are able to describe states both with and without long range order. Both types of LDA states are found [69] to be very low and very close in energy. The lowest energies of LDA and Marshall wavefunctions are about the same.

4. *Two Dimensions—Half Filling*

We turn to the discussion of results for the projected wavefunctions, as they are defined in Section 2.4. In one dim, the Fermi liquid wavefunction, $|\text{Gutz}\rangle$, is the lowest projected wavefunction [36, 39]. In two dimensions, this is no longer the

TABLE II

Results for Two Dimensions

			RVB				
	Gutz	SDW [39]	$\Delta = 0.2$	$\Delta = 1.0$	$\Delta = 2.0$	Mar. [55]	AFH [28]
$\langle \mathbf{S}_i \cdot \mathbf{S}_j \rangle$	-0.267	-0.321	-0.311	-0.318	-0.315	-0.332	-0.334
	± 0.003	± 0.001	± 0.002	± 0.002	± 0.002		± 0.001
M	0.0	0.43	0.0	0.0	0.0	0.36	0.32
$\langle T \rangle$	$-2.65\,t$	$-2.54\,t$	$-2.64\,t$	$-2.44\,t$	$-2.22\,t$	—	—
	$\pm 0.03\,t$	$\pm 0.03\,t$	$\pm 0.05\,t$	$\pm 0.05\,t$	$\pm 0.07\,t$		

Note. The first and second rows show for half filling the nearest-neighbor spin–spin correlation energy in units of $J = 4t^2/U$ and the staggered moment defined by $M^2 = \langle (1/L \sum_i \varepsilon_i \mathbf{S}_i)^2 \rangle$, where $\varepsilon_i = \pm 1$ on the A and B sublattices, respectively. The third row shows the kinetic energy per hole. The first and second columns show the results of the above quantities for the projected Fermi sea, $|\text{Gutz}\rangle$, and for the pojected spin density wave, $|\text{SDW}\rangle$, with an antiferromagnetic order parameter $\Delta_{\text{AF}} = 0.25$. The third, fourth, and fifth columns show the values for the projected BCS wavefunction, $|\text{RVB}\rangle$, with d-wave variational parameters $\Delta = 0.2$, 1.0, and 2.0, respectively. The sixth column shows the results for the best Marshall (Mar.) wavefunction. The last column gives the values obtained by extrapolation of the results obtained by exact diagonalization of H_{eff} (AFH) on small clusters. The numbers in brackets indicate the reference from which the entry is taken.

case. At half filling $|\text{Gutz}\rangle$ is about 20% higher in energy than the best $|\text{RVB}\rangle$ or $|\text{SDW}\rangle$.

In Table II, the extrapolated values for $\langle \mathbf{S}_i \cdot \mathbf{S}_j \rangle$ are shown for $|\text{Gutz}\rangle$, the best $|\text{SDW}\rangle$, and $|\text{RVB}\rangle$ states with $\Delta = 0.2$, 1.0, and 2.0. The renormalized mean field theory [36] indicates $\Delta = 2.0$ as the optimal value, while the MC result gives a somewhat lower energy for $\Delta = 1.0$. Anyhow, the properties of $|\text{RVB}\rangle$ are only weakly dependent on Δ in this parameter region. For comparison, the results for the best Marshall wavefunction [55] and those obtained by extrapolation of the ground state energy of small clusters to the thermodynamic limit [28] are shown.

Two points are to be made. First, both the $|\text{SDW}\rangle$ and the best d-wave $|\text{RVB}\rangle$ gain about 20% in energy with respect to the projected Fermi sea, $|\text{Gutz}\rangle$. For the $|\text{SDW}\rangle$ this might be expected, since this state is constructed explicitly in order to enhance the antiferromagnetic spin–spin correlations.

For the d-wave $|\text{RVB}\rangle$, this large gain is more surprising. A quantum mechanical interference argument can be suggested [68], to give an explanation why it is the d-wave which is favourable in energy. Nevertheless a full understanding of the physics behind this result is still lacking.

Second, although both the $|\text{SDW}\rangle$ and the d-wave $|\text{RVB}\rangle$ are about 5% above the estimated ground state anergy, they are very close in energy. This is remarkable, since their long range behaviours are qualitatively different. The $|\text{SDW}\rangle$ has long range antiferromagnetic order [36], while the $|\text{RVB}\rangle$ has not [40] (see Table II). The same subtle balance between states with and without long range order is present in the class of LDA-wavefunctions [69].

We now discuss results obtained by exact diagonalization of a 10-site cluster [49] by Poilblanc. The exact ground state of this type of cluster has a definite spin (singlet) and space (Γ_2) symmetry [54]. It is straightforward to show that the d-wave $|\text{RVB}\rangle$ fulfills these symmetry requirements, if $a(\mathbf{k}=0) = \infty$ (see discussion in Section 3.3). The $|\text{SDW}\rangle$ on the other hand is not an eigenstate of either symmetry. This different behaviour makes comparison of the $|\text{SDW}\rangle$ and the $|\text{RVB}\rangle$ on small lattices difficult. A correct extrapolation to the thermodynamic limit is therefore essential for reliable results. The lowest RVB-state with real coefficients, $a_{\mathbf{k}}$, has d-wave symmetry. Its energy is 2.2% above the exact ground state energy at half filling. With complex $a_{\mathbf{k}}$ an appreciable lowering of the energy is possible. The full significance of these results for the 10-site cluster had not been worked out at the time of this writing.

5. *Pairing Instabilities in Two Dimensions*

In the preceding section, we described the results for the projected wavefunctions for the half-filled case. We found that the Fermi liquid state is unstable against the introduction of d-wave pairing correlations. We point out by the following short discussion that this effect can be understood already in a Cooper hole analysis. That is, we consider $|\text{Gutz}\rangle$ for the case of two holes, $N = L - 2$, and we examine whether the two holes have the tendency to form a hole–Cooper pair.

On the kind of finite lattice we use, as described in Section 3.5 and illustrated in Fig. 5, the projected Fermi sea, $|\text{Gutz}\rangle$, is uniquely defined in the half-filled case by the prescription to fill consecutively the $\mathbf{k}$-states with lowest $\varepsilon(\mathbf{k}) = -2t(\cos(k_x) + \cos(k_y))$. When we remove two electrons, one with down-spin and one with up-spin, this is no longer the case. A σ-spin can be removed from four different $\mathbf{k}$-states having the same maximal $\varepsilon(\mathbf{k})$. These are the four outermost $\mathbf{k}$-states within the dashed square in Fig. 5.

By combining the four possibilities for the down- and up-spins, respectively, 16 different choices for $|\text{Gutz}\rangle$ are possible, when two holes are present. Out of these 16 states, only 4 have zero total momentum. These are the states, where a $\mathbf{k}, \uparrow$ and a $-\mathbf{k}, \downarrow$ electron are removed at the same time. Only these four states are relevant for the ground state with two holes.

The question whether a coherent superposition of these four states might be lower in energy than the incoherent superposition has been examined by Gros *et al.* [68]. This question is equivalent to the Cooper problem for holes in the context of projected wavefunctions. They found that a superposition with *d*-wave symmetry is favourable, while a superposition with *s*-wave symmetry is higher in energy than the incoherent superposition.

Similar instability considerations can be made for the $|\text{SDW}\rangle$, when two holes are present. The same four possibilities of taking out two electrons with opposite spin and zero total momentum can be considered. In this case, a lowering of the energy by the coherent superposition would indicate coexistence of superconductivity and antiferromagnetism. No such tendency was found [68].

Gros *et al.* [68] also discussed whether the hole–Cooper instability of $|\text{Gutz}\rangle$ could be interpreted by a local hole–hole attraction mechanism. For this purpose, they compared the n.n. hole–hole correlation function in the incoherent and the coherent superpositions, with *d*-wave symmetry, of the four states. They found no enhancement in the latter, within numerical accuracy. They concluded that there was no evidence for a local hole–hole attraction.

This last conclusion must be qualified in view of results for the full *d*-wave RVB-state. In the calculations described above, the s.c. pairing was restricted to the four $\mathbf{k}$-states on the saddle points while all other $\mathbf{k}$-states are either empty or occupied with probability one. In the full $|\text{RVB}\rangle$ states, the whole Brillouin zone is involved in the pairing. In the full wavefunction, the holes are bound in real space, as we show in the next section. This means that the probability of finding two holes on n.n. sites is not only enhanced in a infinite system with respect to the Fermi sea but also finite. The null result for the hole–Cooper problem indicates that for the holes to bind in $|\text{RVB}\rangle$, the whole Brillouin zone must be involved in the pairing of the electrons.

6. *Superconducting Quantum Spin Liquid*

Recently [70], work was begun to distinguish between a "resonating valence bond" (RVB) state and a "quantum spin liquid" (QSL). The notion of a RVB state was

introduced originally [71, 72] for the ground state of a frustrated antiferromagnetic spin system. This term should therefore be most appropriate for a nonordered spin liquid at half filling.

On the other hand, even a nonfrustrated Fermi system becomes paramagnetic, when the doping is large enough (see Section 1.5). In this state the fermionic nature of the spin-carrying particles is essential, since it is their motion which destroys the long range order. That is what one might call a QSL. Note that at half filling, the Fermi character of the spin-carriers is lost, since they cannot move. All physical quantities can be expressed in terms of spin operators, like $S_i^+ S_j^-$. For the projected wavefunction, the situation is special isofar as the trial wavefunction for a QSL evolves continuously from the trial wavefunction for a RVB state, just by the introduction of holes. The name $|\mathrm{RVB}\rangle$ will therefore be kept.

We now discuss the results for the d-wave $|\mathrm{RVB}\rangle$, which is our trial wavefunction for a QSL, since it is the lowest [36, 40] of the projected wavefunctions as defined in Section 2.4. The optimal value for Δ varies between 0.5 and 2.0, depending on the doping and the ratio of t/J in H_{eff}. The qualitative properties of this state however do not depend crucially on the exact value of Δ.

Off half filling, three terms contribute to $\mathrm{H_{eff}}$. For a system with $L=82$ sites, $N_h=8$ holes, and $U=16t$, the total energy has been calculated [40]. A minimum for $\Delta \sim 0.55$ has been found, which is due to the gain in spin correlation energy. The kinetic energy instead is reduced with respect to its value at $\Delta=0$ (see Table II). Note that the kinetic energy for the d-wave $|\mathrm{RVB}\rangle$ drops very fast around $\Delta \sim 1.0$, while $\langle \mathbf{S}_i \cdot \mathbf{S}_j \rangle$ has a broad minimum around the same value of Δ.

We now discuss the hole–hole correlation function, which is defined by

$$g_{\mathbf{T}} = \frac{1}{(1-n)^2} \frac{1}{L} \sum_{\mathbf{R}} \langle (1-n_{\mathbf{R},\downarrow})(1-n_{\mathbf{R},\uparrow})(1-n_{\mathbf{R}+\mathbf{T},\downarrow})(1-n_{\mathbf{R}+\mathbf{T},\uparrow}) \rangle, \qquad (32)$$

where $\mathbf{T}$ is a lattice vector and $n_{\mathbf{R},\sigma} = c^+_{\mathbf{R},\sigma} c_{\mathbf{R},\sigma}$. The results are given in Table III, for the d-wave $|\mathrm{RVB}\rangle$ with $\Delta=2.0$. The data shown are obtained by average of Eq. (32) over the four $\mathbf{T}$'s, which can be obtained by rotation by $\pi/2$.

In order to give an impression of the accuracy and the computation time needed, both are given in Table III. Also shown is the acceptance rate, i.e., the average of $T(\alpha \to \alpha')$ (see Section 3.1). The configurations α and α' differ here by the interchange of two n.n. electrons with opposite spin or by the interchange of an electron and a n.n. empty site.

The normalization factor $1/(1-n)^2$ in the definition of $g_{\mathbf{T}}$ has the following meaning: If the empty sites would be completely uncorrelated, i.e., randomly distributed, $g_{\mathbf{T}}$ would be identically 1, independent of $\mathbf{T}$. For a finite system, the normalization factor is replaced by $L(L-1)/(N_h(N_h-1))$.

If the holes behaved like weakly interacting fermions, or like bosons with short range repulsion, $g_{\mathbf{T}}$ would be smaller than 1 for small distances and go to 1 at large distances. This behaviour is found for $|\mathrm{Gutz}\rangle$ [8] (see Fig. 6). For the $|\mathrm{RVB}\rangle$

TABLE III

Hole–Hole Correlations

	26	50	82	122	170	226	$p_{\mathbf{T}}^{\Delta=2.0}$	$p_{\mathbf{T}}^{\Delta=0.2}$
(0, 1)	1.06 ±0.01	1.23 ±0.02	1.48 ±0.03	1.76 ±0.06	2.13 ±0.13	2.42 ±0.19	0.097	0.023
(1, 1)	1.06 ±0.01	1.22 ±0.01	1.44 ±0.02	1.65 ±0.06	2.01 ±0.13	2.27 ±0.15	0.086	0.024
(0, 2)	0.94	0.85	0.81	0.75	0.71	0.69	0.000	—
(1, 2)	0.98	0.99	0.98	1.02	1.06	1.11	0.001	—
(2, 2)	0.97	0.94	0.90	0.86	0.79	0.72	0.000	—
N_{MC}/L	24 000	24 000	12 000	4 800	2 400	1 200		
Accept.	0.34	0.26	0.20	0.17	0.15	0.14		
Time (min)	6	23	36	40	49	55		

Note. The first five rows and six columns show $g_{\mathbf{T}}$ for systems with eight holes in $L = 26, 50, 82, 122, 170, 226$ sites, for the d-wave $|\mathrm{RVB}\rangle$ with $\Delta = 2.0$ and $\mathbf{T} = (0, 1), (1, 1), (0, 2), (1, 2), (2, 2)$. For $\mathbf{T} = (0, 1), (1, 1)$ the accuracy of the calculation is given; for the other values of $\mathbf{T}$ they are roughly the same. The seventh and eighth columns show $p_{\mathbf{T}}$, the probabilities of finding two holes in relative positions $\mathbf{T}$, obtained by a linear fir of g_T versus L. The sixth row gives the number of MC updatings; the total number of MC steps (N_{MC}) where L times as large. The seventh row shows the acceptance rate (Accept.) for the same calculation. The total time for the program to run on a Cray 1 – s (of the EPFL Lausanne) is given in minutes in the last row.

wavefunction, the situation is completely different. The holes are found to be bound.

To see this, we define $p_{\mathbf{T}}$ to be the probability of finding an pair of holes in a state with relative positions $\pm\mathbf{T}$. With N_h holes, when $N_h \ll L$, the number of pairs in a state with relative positions $\pm\mathbf{T}$ is at any given moment $N_h p_{\mathbf{T}}$. Then, $g_{\mathbf{T}}$ takes the value $0.5(L-1)(N_h-1)^{-1}p_{\mathbf{T}}$.

We have done the calculation with a fixed number of holes; $g_{\mathbf{T}}$ should therefore increase linearly with L, whenever $p_{\mathbf{T}}$ is finite. From Fig. 6 we see that this is the case for the d-wave $|\mathrm{RVB}\rangle$ and $\mathbf{T} = (0, 1)$, while $g_{(0,1)}$ goes to a constant for the Fermi liquid state ($\Delta = 0$). We conclude, that in $|\mathrm{RVB}\rangle$ the holes are bound, but not in $|\mathrm{Gutz}\rangle$. From a linear fit of $g_{\mathbf{T}}$, the value of $p_{\mathbf{T}}$ can be extracted. The results are given in Table III.

The results can be understood in the following way: If we consider two holes in the thermodynamic limit, then the probability of finding the two holes on n.n. sites is $2 \cdot p_{(0,1)} \sim 20\%$ and on n.n.n. sites $2 \cdot p_{(1,1)} \sim 19\%$. On the other hand, $p_{(0,2)}$ and $p_{(2,2)}$ vanish, indicating a node of the hole–hole pair wavefunction at these points. We find therefore an overall probability of about 40% to find the two holes within two to three lattice constants. Note that this probability is reduced to $\sim 10\%$ for $\Delta = 0.2$.

The interpretation of these results is difficult. In particular, it is not clear whether this binding of the holes can be interpretated as due to a local attraction of holes.

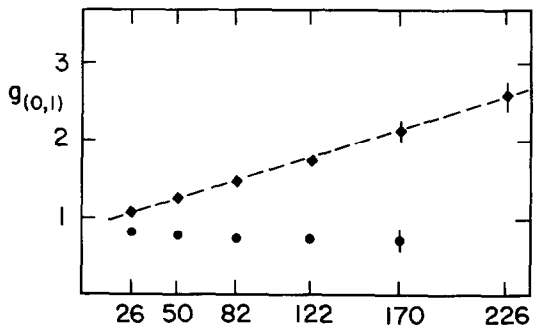

FIG. 6. The nearest-neighbour hole–hole correlation function $g_{(0,1)}$, as defined by Eq. (32). The calculations were done for a fixed number of eight holes and lattices with a total number of $L = 26$, 50, 82, 122, 177, 226 sites. The solid squares give the results for the d-wave |RVB⟩ for $\Delta = 2.0$ (see Table III). The dashed line is a linear fit to the data. The filled circles are the data points for |Gutz⟩, the projected Fermi sea. Note that the data points for |RVB⟩ increase linearly, indicating bound holes, while the data for |Gutz⟩ go to a constant for $L \to \infty$.

A possible binding of two holes is a background with antiferromagnetic correlations, due to the formation of a spin bag with ferromagnetic tendency (see the discussion of the *Nagaoka* effect in Section 1.5), has been proposed in the case of strong [73] and weak [74] coupling. A similar mechanism of a local hole–hole attraction in a three band model for the Cu–O layer of high T_C compounds has also been investigated [75, 76].

In any case, we do not yet understand why the |RVB⟩ wavefunctions, which have built in explicitly only superconducting correlations between electrons, yield automatically bound empty sites.

One has two possibilities to numerically investigate whether the |RVB⟩ state is really superconducting. One is to directly evaluate the quantity $\langle c^+_{i,\uparrow} c^+_{j,\downarrow} \rangle$, where $\langle i, j \rangle$ are n.n. sites. This quantity has been proposed as the s.c. order parameter in various mean field approaches [36, 40, 43–45]. It has also been calculated numerically [40]. It is found to be different from zero for finite hole concentrations and to vanish like $(1 - n)$ as $n \to 1$.

The second possibility is to calculate directly the "off diagonal long range order" (ODLRO). This quantity can be defined for Fermions as [77]

$$\lim_{|\mathbf{R}-\mathbf{R}'| \to \infty} \langle c^+_{\mathbf{R},\uparrow} c^+_{\mathbf{R}+\mathbf{T},\downarrow} c_{\mathbf{R}'+\mathbf{T}',\downarrow} c_{\mathbf{R}',\uparrow} \rangle, \tag{33}$$

where $\mathbf{T}, \mathbf{T}' = (1, 0), (0, 1)$. ODLRO means that the quantity defined by Eq. (33) is finite in the thermodynamic limit. Yang [77] has shown that a state with ODLRO shows flux quantization with a flux quanta of $hc/2e$. Such a state would therefore be superconducting. Physically this means that pairs of electrons can hop coherently over infinite distances, i.e., that they are Bose condensed.

The direct calculation of this quantity is difficult, since the extrapolation $|\mathbf{R}-\mathbf{R}'| \to \infty$ is difficult to perform. We have therefore calculated the quantity

$$\phi = \frac{1}{(1-n)^2} \left\langle \left(\frac{1}{L} \sum_{\mathbf{R},\mathbf{T}=(1,0),(0,1)} c^{+}_{\mathbf{R},\uparrow} c^{+}_{\mathbf{R}+\mathbf{T},\downarrow} (\pm 1)^{T_y} \right) \cdot \left(\frac{1}{L} \sum_{\mathbf{R}',\mathbf{T}'=(1,0),(0,1)} c_{\mathbf{R}'+\mathbf{T}',\downarrow} c_{\mathbf{R}',\uparrow} (\pm 1)^{T'_y} \right) \right\rangle. \tag{34}$$

Here $\mathbf{T} = (T_x, T_y)$, $(\pm 1) \to (+1)$ for s-wave symmetry in $|\mathrm{RVB}\rangle$ and $|\mathrm{Gutz}\rangle$, and $(\pm 1) \to (-1)$ for the d-wave $|\mathrm{RVB}\rangle$. A finite ϕ in the thermodynamic limit implies ODLRO, since for $L \to \infty$ only the terms with large separation between $\mathbf{R}$ and $\mathbf{R}'$ contribute to ϕ.

We have calculated ϕ for a fixed number of eight holes and varying lattice sizes. The results are shown in Fig. 7. We see that ϕ vanishes like $1/L$ for the projected Fermi sea, $|\mathrm{Gutz}\rangle$. This is to be expected; no s.c. can be present in a Fermi liquid state. For the d-wave $|\mathrm{RVB}\rangle$, ODLRO is present in the thermodynamic limit. ϕ is increasing linearly, because of the normalization factor $(1-n)^{-2}$ of the definition. If the holes were not bound, ϕ would go to a constant for $L \to \infty$.

We have therefore proven that the $|\mathrm{RVB}\rangle$ wavefunctions are indeed s.c. off half filling. This is of course not yet a proof that the ground state of H_{eff} is s.c. for $n \ll 1$. In fact, results from quantum Monte Carlo simulations at high temperatures [78] challenge these findings. Within this approach by projected wavefunctions, a QSL is therefore intrinsically superconducting. This differs from the approach by

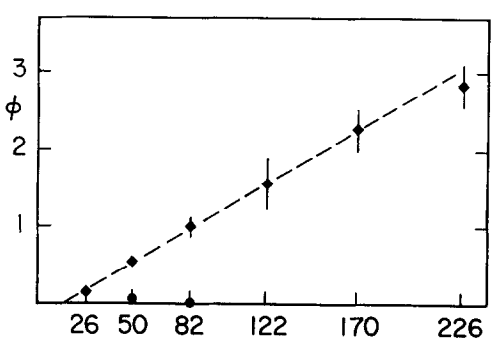

FIG. 7. The quantity ϕ as defined by Eq. (34). The calculations were done for a fixed number of eight holes and lattices with a total number of $L = 26$, 50, 82, 122, 177, 226 sites. The solid squares give the results for the d-wave $|\mathrm{RVB}\rangle$ for $\Delta = 2.0$. The solid circles are the data points for $|\mathrm{Gutz}\rangle$, the projected Fermi sea. A finite ϕ in the thermodynamic limit means "off diagonal long range order" (ODLRO). Because of the normalization in the definition, ϕ actually increases linearly with L for the d-wave projected BCS wavefunction, since the holes are bound in this wavefunction (see Fig. 6). For the projected Fermi sea, ϕ vanishes like $1/L$; no superconductivity is present. Since the data points can barely be seen on this scale, we give them explicitly for $L = 26$, 50, and 82: 0.105 ± 0.019, 0.054 ± 0.009, and 0.043 ± 0.015.

Wheatly *et al.* [79], which regard the QSL only as a background for pair condensation for Bose holes coupled due to interlayer hopping.

7. *Summary*

We examined the properties of projected wavefunctions in one and two dimensions. In one dimension we compared the projected Fermi sea with the known exact ground state. We have found close qualitative and quantitative agreement. For less than one particle per site the projected Fermi sea has Fermi liquid character. We conclude that it is therefore possible to describe a nearly localized Fermi liquid by a projected Fermi sea.

In two dimensions, we discussed the projected wavefunctions in view of the interplay of short and long ranged antiferromagnetism. While the latter dominates near half filling, a quantum spin liquid is expected to take over at a small but finite hole concentration. We calculated the properties of the projected BCS wavefunction with d-wave symmetry and found it to be a good candidate of the ground state of a quantum spin liquid. This state is superconducting off half filling. We calculated the superconducting order parameter and confirmed that it has d-wave symmetry. We believe that the results are of importance for an understanding of the Cu–O superconductors, since neutron scattering data indicate [2] that such a state is indeed realized in these compounds.

ACKNOWLEDGMENTS

I thank T. M. Rice for support and collaboration. I am grateful to C. Bruder, F. C. Zhang, and D. Poilblanc for stimulating discussions. The support of the Swiss Nationalfond is gratefully acknowledged.

REFERENCES

1. P. W. ANDERSON, *Science* **235** (1987), 1196.
2. R. J. BIRGENEAU, D. R. GABBE, H. P. JENSSEN, M. A. KASTNER, P. J. PICONE, T. R. THURSTON, G. SHIRANE, U. ENDOH, M. SATO, K. YAMADA, Y. HIDAKA, M. ODA, Y. ENOMOTO, M. SUZUKI, AND T. MURAKAMI, *Phys. Rev. B* **38** (1988), 6614.
3. J. E. HIRSCH, *Phys. Rev. B* **31** (1985), 4403.
4. Sir N. MOTT, *Philos. Mag. B* **50** (1984), 161.
5. W. KOHN, *Phys. Rev. A* **133** (1964), 171.
6. H. Q. LIN AND J. E. HIRSCH, *Phys. Rev. B* **35** (1987), 3359.
7. Y. NAGAOKA, *Phys. Rev.* **147** (1966), 392.
8. T. EINNARSON, Diplomarbeit, ETH-Zürich, WS 1986/87.
9. W. E. BRINKMAN AND T. M. RICE, *Phys. Rev. B* **2** (1970), 1324.
10. C. GROS, R. JOYNT, AND T. M. RICE, *Phys. Rev. B* **36** (1987), 381.
11. E. H. LIEB AND F. Y. WU, *Phys. Rev. Lett.* **20** (1968), 1445.
12. N. D. MERMIN AND H. WAGNER, *Phys. Rev. Lett.* **17** (1966), 1133.
13. P. C. HOHENBERG, *Phys. Rev.* **158** (1967), 383.
14. J. KANAMORI, *Prog. Theor. Phys.* **30** (1963), 275.
15. P. W. ANDERSON, *Phys. Rev.* **115** (1959), 2.

16. (a) J. HUBBARD, *Proc. R. Soc. London A* **276** (1964), 238; (b) **285** (1965), 542.
17. T. V. RAMAKRISHNAN AND B. S. SHASTRY, to be published.
18. H. SHIBA, *Phys. Rev. B* **6** (1972), 930.
19. J. CARMELO AND D. BAERISWYL, *Phys. Rev. B* **33** (1988), 7247.
20. H. J. SCHULZ, *Europhys. Lett.* **4** (1987), 609.
21. K. KUBO AND M. TADA, *Prog. Theor. Phys.* **71** (1984), 479.
22. B. H. ZHAO, H. Q. NIE, K. Y. ZHANG, K. A. CHAO, AND R. MICNA, *Phys. Rev. B* **36** (1987), 2321.
23. J. E. HIRSCH, *J. Stat. Phys.* **43** (1986), 841.
24. R. T. SCALETTAR, D. J. SCALAPINO, AND R. L. SUGAR, *Phys. Rev. B* **34** (1986), 7911; (b) M. IMADA, *J. Phys. Soc. Japan* **57** (1988), 42; (c) I. MORGENSTERN, *Z. Phys. B* **70** (1988), 279.
25. M. TAKAHASHI, *Phys. Soc. Japan* **51** (1982), 3475.
26. A. REICH AND L. M. FALICOV, *Phys. Rev. B* **36** (1987), 3117.
27. J. OITMAA AND D. D. BETTS, *Canad. J. Phys.* **56** (1978), 897.
28. D. A. HUSE, *Phys. Rev. B* **37** (1988), 2380.
29. (a) J. D. REGER AND A. P. YOUNG, *Phys. Rev. B* **37** (1988), 5978; (b) T. BARNES AND E. SWANSON, *Phys. Rev. B* **37** (1988), 9405.
30. M. C. GUTZWILLER, *Phys. Rev. Lett.* **10** (1963), 159.
31. T. A. KAPLAN, P. HORSCH, AND P. FULDE, *Phys. Rev. Lett.* **49** (1982), 889.
32. M. GUTZWILLER, *Phys. Rev. B* **137** (1965), A1726.
33. T. M. RICE AND K. UEDA, *Phys. Rev. Lett.* **55** (1985), 995.
34. M. ROOS, private communication.
35. G. KOTLIAR AND A. E. RUCKENSTEIN, *Phys. Rev. Lett.* **57** (1985), 1362.
36. F. C. ZHANG, C. GROS, T. M. RICE, AND H. SHIBA, *Supercond. Sci. Technol.* **1** (1988), 36.
37. W. METZNER AND D. VOLLHARDT, *Phys. Rev. Lett.* **59** (1987), 121.
38. F. GEBHARDT AND D. VOLLHARDT, *Phys. Rev. Lett.* **59** (1987), 1472.
39. H. YOKOYAMA AND H. SHIBA *J. Phys. Soc. Japan* **56** (1987), 3570.
40. C. GROS, *Phys. Rev. B*, **38** (1988), 931.
41. G. BASKARAN, Z. ZOU, AND P. W. ANDERSON, *Solid State Commun.* **63** (1987), 973.
42. H. YOKOYAMA AND H. SHIBA, *J. Phys. Soc. Japan* **57** (1988), 2482.
43. G. KOTLIAR, *Phys. Rev. B* **37** (1988), 3664.
44. A. E. RUCKENSTEIN, P. J. HIRSCHFELD, AND J. APPEL, *Phys. Rev. B* **36** (1987), 857.
45. I. AFFLECK AND J. B. MARSTON, *Phys. Rev. B* **37** (1988), 3774.
46. P. HORSCH AND T. A. KAPLAN, *J. Phys. C* **16** (1983), L1203.
47. H. SHIBA, *J. Phys. Soc. Japan* **55** (1986), 2765.
48. J. P. BOUCHAUD, A. GEORGES, AND C. LHUILLER, *J. Phys. (Paris)* **49** (1988), 553.
49. D. POILBLANC, to be published.
50. D. CEPERLY, G. V. CHESTER, AND M. H. KALOS, *Phys. Rev. B* **16** (1977), 3081.
51. P. HORSCH AND T. A. KAPLAN, *Bull. Amer. Phys. Soc.* **30** (1985), 513.
52. H. YOKOYAMA AND H. SHIBA, *J. Phys. Soc. Japan* **56** (1987), 1490.
53. H. YOKOYAMA AND H. SHIBA, *J. Phys. Soc. Japan* **56** (1987), 3582.
54. W. MARSHALL, *Proc. R. Soc. London A* **232** (1955), 48.
55. D. HUSE AND V. ELSER, *Phys. Rev. Lett.* **60** (1988), 2531.
56. P. HORSCH AND W. VON DER LINDEN, *Z. Phys. B* **72** (1988), 181.
57. P. TAVAN, *Z. Phys. B* **72** (1988), 277.
58. A. LUTHER AND I. PESCHEL, *Phys. Rev. B* **12** (1975), 3908.
59. B. S. SHASTRY, *Phys. Rev. Lett.* **60** (1988), 639.
60. D. HALDANE, *Phys. Rev. Lett.* **60** (1988), 635.
61. T. K. LEE, W. VON DER LINDEN, AND P. HORSCH, *in* "Proceedings of the International Conference on High-Temperature Superconductors and Materials and Mechanism of Superconductivity," *Physica C* **153** (1988), 155.
62. J. DES CLOISEAUX AND J. J. PEARSON, *Phys. Rev.* **128** (1962), 2131.
63. R. B. GRIFFITHS, *Phys. Rev.* **133** (1964), A768.

64. J. M. LUTTINGER, *Phys. Rev.* **119** (1960), 1153.
65. P. A. LEE, T. M. RICE, J. W. SERENE, L. J. SHAM, AND J. W. WILKINS, *Comments Condens. Mater Phys.* **12** (1986), 99.
66. T. M. RICE, K. UEDA, H. R. OTT, AND H. RUDIGER, *Phys. Rev. B* **31** (1985), 594.
67. K. SEILER, C. GROS, T. M. RICE, K. UEDA, AND D. VOLLHARDT, *J. Low Temp. Phys.* **64** (1986), 195.
68. C. GROS, R. JOYNT, AND T. M. RICE, *Z. Phys. B* **68** (1987), 425.
69. S. LIANG, B. DOUCOT, AND P. W. ANDERSON, *Phys. Rev. Lett.* **61** (1988), 365.
70. C. GROS, D. POILBLANC, T. M. RICE, AND F. C. ZHANG, *in* "Proceedings of the International Conference on High-Temperature Superconductors and Materials and Mechanism of Superconductivity," in press.
71. P. W. ANDERSON, *Mater. Res. Bull.* **8** (1973), 153.
72. P. FAZEKAS AND P. W. ANDERSON, *Philos. Mag.* **30** (1974), 474.
73. Y. TAKAHASHI, *Z. Phys. B* **67** (1987), 503.
74. J. R. SCHRIEFFER, X. G. WENG, AND S. C. ZHANG, *Phys. Rev. Lett.* **60** (1988), 944.
75. A. AHARONY, R. J. BIRGENAU, A. CONIGLIO, M. A. KASTNER, AND H. E. STANLEY, *Phys. Rev. Lett.* **60** (1988), 1330.
76. M. OGATA AND H. SHIBA, to be published.
77. C. N. YANG, *Rev. Mod. Phys.* **34** (1962), 694.
78. J. E. HIRSCH, E. LOH, D. J. SCALAPINO, AND S. TANG, *in* "Proceedings of the International Conference on High-Temperature Superconductors and Materials and Mechanism of Superconductivity," in press.
79. J. M. WHEATLY, T. C. HSU, AND P. W. ANDERSON, *Phys. Rev. B* **37** (1988), 5897.